GENE EXPRESSION PROFILING OF MYOSTATIN NULL MICE

BY

SAVANNAH GABRIEL

THESIS

Submitted in partial fulfillment of the requirements
for the degree of Master of Science in Animal Sciences
in the Graduate College of the
University of Illinois at Urbana-Champaign, 2009

Urbana, Illinois

Adviser:

Professor John Killefer

ABSTRACT

Increasing muscle growth is beneficial to the meat animal industry and for biomedical research. Altering myostatin function and administration of β-adrenergic agonists, such as clenbuterol, enhances muscle growth. However, it is unclear whether the mechanisms of these effects converge in a single pathway. Previous work demonstrated that myostatin null mice (MKO) did respond to clenbuterol with increased body and muscle weights suggesting disparate mechanisms for each effect. We examined gene expression profiles of these mice to identify downstream targets of myostatin null- and clenbuterol-induced skeletal muscle hypertrophy. Microarray analysis was not successful at identifying gene expression differences between clenbuterol-treated and control mice. Differences in gene expression between the MKO mice and wild type (WT) mice were observed including changes in genes related to amino acid and derivative metabolism - specifically creatine biosynthesis and metabolism, development, muscle contraction, transport, and Wnt receptor signaling. Real Time PCR (RT-PCR) was employed to validate genes associated with each of these processes in the tibialis anterior, gastrocnemius, and soleus muscles. Additionally, creatine content and creatine kinase (CK) activity was directly measured in the tibialis anterior and gastrocnemius muscles. Expression of nearly all genes investigated was consistent with microarray analysis, as was expression of myosin heavy chain isoforms. Furthermore, creatine and creatine kinase activity were increased in myostatin null mice compared with wild type mice. Therefore this experiment confirms the role of myostatin as a negative regulator of muscle mass and also demonstrates some of the downstream effects of skeletal muscle hypertrophy associated with the myostatin null mutation.

ACKNOWLEDGEMENTS

First I must thank Dr. John Killefer who has been my adviser for the past six years and has always supported me throughout my career at the University of Illinois. I also want to thank the past and present members of the Meat Science Laboratory- students and professors included. I consider them all my family and I am very grateful to have shared academic and life experiences with each one of them. I want to thank Anna Dilger for all of her guidance and support and her friendship. She has helped make this thesis what it is and I truly appreciate everything she has done for it- and for me. To Dustin Boler and Chad Souza- thank you for all of your help with classes and for always providing me with a laugh. I want to give credit to Lou Kutzler who helped me out tremendously with mouse work. I must also give credit to my parents for always allowing me to choose my own path and make my own decisions- and my own mistakes. I always learn from them- just like you told me I would. To my sisters, Nicole and Chelsea- you are truly my best friends and your faith in me has helped in so many ways. To my brother, Aaron, thank you for protecting our country and supporting me in my academic career- I look forward to supporting you in yours one day. To my great-grandmother, I have missed your "letters from Dorothy" these past three years, but your kind words of love and encouragement will always stay with me. To my future husband- Sean Holmer- thank you for helping me stay on track and stay motivated. You are the most ambitious person I know and I just hope I can keep up with you for the rest of my life. Most of all, I must thank God for the many blessings He has provided. I look forward to the blessings of the future.

TABLE OF CONTENTS

Chapter **Page**

I. REVIEW OF THE LITERATURE 1
Myogenesis 1
Post-natal Muscle Growth 3
Muscle Fiber Types 7
Objectives 9
Techniques for Identifying Pathways of Muscle Hypertrophy....10
Literature Cited....16

II. GENE EXPRESSION PROFILING OF WILD TYPE AND MYOSTATIN NULL MICE TREATED WITH CLENBUTEROL 24
Abstract....24
Introduction....24
Materials and Methods 27
Results and Discussion 30
Conclusions....35
Literature Cited....37
Tables and Figures....41

III. CHANGES IN GENE EXPRESSION, CREATINE CONTENT AND ENZYME ACTIVITY IN MYOSTATIN NULL MICE AND WILD TYPE MICE ….....48
Abstract....48
Introduction....49
Materials and Methods 51
Results and Discussion 54
Conclusions....59
Literature Cited....61
Tables and Figures....65

APPENDIX....70
List of genes for Gene Ontology Tree Machine Annotation 70

AUTHOR'S BIOGRAPHY....76

CHAPTER 1

REVIEW OF THE LITERATURE

Different hypertrophic mechanisms in muscle, while they may involve divergent upstream pathways, should ultimately converge on a common final set of processes. Identifying these processes, common genes, and transcripts would be beneficial to both animal agriculture and human biomedical research. Alterations in myostatin functionality and administration of the β-adrenergic agonist clenbuterol have been well characterized for inducing skeletal muscle hypertrophy; however, the exact mechanisms behind these actions remain unclear. This review will focus on muscle development, growth, and protein accretion with an emphasis on increasing muscle mass specifically by altering myostatin function or by clenbuterol administration. It will also discuss microarray technology and quantitative real-time polymerase chain reaction (RT-PCR), two useful techniques for determining the physiological functions of myostatin and clenbuterol.

Myogenesis

Embryonic formation of muscle fibers, or myogenesis, begins with mesenchymal precursor cells. These cells first commit to the myogenic lineage by expressing muscle regulatory factors (MRFs) and proliferate, forming a pool of myoblasts. The purpose of MRFs is to stop proliferation and induce differentiation. Expression of the transcription factor, Pax3, promotes expression of these myogenic differentiation factors, including MyoD and Mrf5 (Williams and Ordahl, 1994). MyoD up-regulates p21, a cyclin dependent kinase inhibitor that prevents phosphorylation of the retinoblastoma protein (Rb) (Sherr and Roberts, 1999). Phosphorylated Rb (pRb) inhibits cell cycle progression.

Myoblasts then withdraw from the cell cycle and are terminally differentiated. Myoblasts fuse to form myotubes with centralized nuclei, and they accumulate myofibrils (contractile apparatus) and mature into functional muscle cells.

Myostatin and myogenesis

Myostatin is a key regulator of skeletal muscle growth and development and is a member of the transforming growth factor-β (TGF-β) superfamily. It negatively regulates skeletal muscle mass. Myostatin possesses the characteristics of the TGF-β superfamily in that it is secreted as a latent complex. Myostatin circulates in its latent form in both mouse and human serum (Hill et al., 2002). In order for myostatin to be active, the inactive N-terminal signaling sequence, the propeptide, must first be cleaved from the C-terminal region. A second proteolytic cleavage frees the active C-terminal fragment which allows receptor binding (McPherron, et al., 1997).

Myostatin function is highly conserved across vertebrate species (McPherron et al., 1997). Mutations of the gene result in hyper-muscular phenotypes observed in cattle (Grobet et al., 1997; 1998; McPherron & Lee, 1997), humans (Schuelke et al., 2004), sheep (Clop et al., 2006) and dogs (Mosher et al., 2007). Animals without functional myostatin exhibit primarily hyperplasia- an increase in the number of muscle fibers and to a lesser extent hypertrophy- an increase in the size of muscle fibers (McPherron & Lee, 1997).

The inhibitory effect of myostatin on muscle growth begins during myogenesis. In vitro studies of C_2C_{12} myoblasts treated with exogenous myostatin demonstrated significant up-regulation of p21 (Thomas et al., 2000) and reduced DNA synthesis (Taylor et al., 2001) suggesting myostatin inhibits myoblast proliferation. Myostatin also

inhibits differentiation. Significant up-regulation of myostatin mRNA is observed during myogenic differentiation (Rios et al., 2002). Myostatin inhibits MyoD expression (Langley et al., 2002), and down-regulates expression of other components of differentiation such as myogenin, downstream targets of myogenic differentiation factors, and creatine kinase (Ríos et al., 2001). Conversely, double-muscled cattle fetuses exhibit increased expression of MyoD and increased differentiation in the absence of myostatin (Oldham et al., 2001). Thus, functional myostatin inhibits both myoblast proliferation and differentiation, and the loss of myostatin function as in myostatin null mice results in the opposite effect: increased muscle hyperplasia (McPherron & Lee, 1997).

Post-natal Muscle Growth

Protein accretion

Because the number of skeletal muscle fibers is largely fixed at birth, postnatal muscle growth generally occurs via two mechanisms: by hypertrophy, the increase in size of muscle fibers, and by the accretion of material between cells. Hypertrophy of muscle fibers is a result of the deposition of additional muscle protein and incorporation of more nuclei into the multi-nucleated muscle fiber. Skeletal muscles grow in length via the addition of sarcomeres in response to stretch, and in width via the addition and/or splitting of myofibrils in response to work. Both of these processes require increased protein accretion. Protein accretion occurs when protein synthesized exceeds protein degraded; therefore protein accretion occurs as a result of increased synthesis and/or decreased degradation. Protein synthesis occurs through signaling from various pathways including but not limited to insulin-like growth factor signaling, the PI3K-Akt-mammalian target of rapamycin (mTOR) pathway, and through glycogen synthase kinase

3 β (GSK-3β) (reviewed by Glass, 2003). Protein degradation in skeletal muscle is mediated by calcium-dependent activation of calpains, ATP-dependent ubiquitination, lysosomal proteases, and apoptosis (Glass, 2003).

In addition to its role in embryonic myogenesis, myostatin plays an important role in muscle growth throughout the life of an animal. The myostatin protein is first detected in mouse embryos, and expression persists through adulthood (McPherron et al., 1997). Also, myostatin null mice retain their hyper-muscular phenotypes even with aging in contrast to normal mice (Wagner et al., 2005). Postnatal expression of myostatin propeptide cDNA has also been shown to maintain high muscle growth (Yang et al., 2001). Recently, myostatin has been implicated as a negative regulator of the Akt/mTOR pathway (Amirouche et al., 2009). This result has been confirmed with microarray experiments which identify components of the PI3K/Akt/GSK-3β as up-regulated in myostatin null mice (Chelh et al., 2009). This introduces a new role for myostatin in the regulation of protein synthesis and confirms its important function in adult skeletal muscle.

Myostatin is also involved in muscle atrophy and increased protein degradation. For instance, patients with HIV express higher levels of myostatin in conditions of muscle wasting (Gonzalez-Cadavid et al., 1998). Additionally, cachexia is induced in animals over-expressing myostatin (Zimmers et al., 2002). Conversely, administration of a myostatin antibody to dystrophic mice increases body and muscle weights while simultaneously reducing muscle degeneration and increasing levels of creatine kinase (Bogdanovich et al., 2002). Myostatin has been shown to induce atrophy by up-regulating genes involved in ubiquitin-mediated proteolysis (McFarlane et al., 2006).

Another way to alter postnatal muscle protein accretion is use of β-adrenergic agonists (BAA) stimulating β-adrenoreceptors (B-AR), which are distributed differently but present in nearly all cell types. Three subtypes of B-AR are present in skeletal muscle, β1, β2, and β3, but the β2 subtype is present in the greatest proportion (Williams et al., 1984; Kim & Sainz, 1992) and may be most responsible for skeletal muscle hypertrophy (Hinkle et al., 2002). Clenbuterol is a synthetic BAA that stimulates β2 B-AR and increases muscle mass in numerous species such as mice, rats, cattle, chickens, pigs, and sheep (reviewed by Ricks et al., 1984). The primary mechanism of action is to increase levels of cyclic AMP (cAMP) with subsequent activation of protein kinase A (reviewed by Mersmann, 1998). Protein kinase A then activates several down-stream targets responsible for altering protein accretion.

One proposed downstream target of clenbuterol is insulin-like growth factors (IGF), which have been well characterized for their roles in protein synthesis and translation as well as myogenesis (reviewed by Jones & Clemmons, 1995). Administration of clenbuterol causes a transient increase of IGF-I in cells (Awede et al., 2002) and of IGF-II in rat soleus (Sneddon, et al., 2001) and masseter muscles (Matsumoto et al., 2006). Clenbuterol, like other BAA, also activates the phosphoinositol 3-kinase (PI3K) - Akt signaling pathway (Schmidt et al., 2001; Kline et al., 2007) which is responsible for protein synthesis and proteolysis. Greater RNA accretion and total translational capacity is also observed in animals administered clenbuterol (Maltin et al., 1987), suggesting clenbuterol increases protein synthesis.

Clenbuterol also inhibits protein degradation as demonstrated in muscle wasting studies (Zeman et al., 1987; Zeman et al., 2000). Lambs fed clenbuterol exhibit increased

concentrations of calpains and calpastatin (Higgins et al., 1988). As further support of clenbuterol's role in calcium-dependent proteolysis, Navegantes and colleagues (Navegantes et al., 2001) showed that clenbuterol inhibits Calcium-dependent proteolysis in rat muscles. Clenbuterol has also been implicated in ATP-dependent proteolysis as rats treated with clenbuterol have reduced expression of ubiquitin mRNA (Costelli et al., 1995). This effect was recently confirmed in a study that clenbuterol suppressed E3 ubiquitin ligases (Kline et al., 2007). The anabolic effects of clenbuterol are more prevalent in fast- twitch muscle fibers (Kim & Sainz, 1992), and it has been shown that clenbuterol inhibits ubiquitination in fast muscles more completely than in slow muscles (Yimlamai et al., 2005).

Satellite cells

Though protein accretion occurs throughout muscle growth, the DNA: protein ratio of muscle cells is relatively constant, suggesting an increase in nuclei. Because mature muscle cells are post-mitotic and unable to divide, they must acquire external DNA. Unlike adult muscle cells, satellite cells retain their mitotic capacity and serve as myonuclei necessary for muscle growth, repair, and regeneration (Mauro, 1961). As animals age, however, the satellite cell population decreases in absolute number and as a percentage of nuclei in skeletal muscle tissue (Snow, 1977). The distribution of satellite cells also varies among muscle fiber types with slow muscle fibers having a greater proportion than fast muscle fibers (reviewed by Chen & Goldhamer, 2003). Satellite cells, in a similar manner to embryonic myoblasts, undergo multiple rounds of division prior to terminal differentiation and fusion to form multinucleated myofibers by mechanisms which are not clear (McKinnell et al., 2005). Unlike myoblasts, however,

satellite cells maintain their ability to self-renew by generating identical daughter cells to restore the pool of quiescent satellite cells in a process called asymmetric division (Kuang et al., 2007).

Myostatin is expressed in satellite cells and regulates satellite cell quiescence and self-renewal (Cornelison et al., 2000). Higher levels of myostatin have been observed in quiescent satellite cells and lower levels are observed when satellite cells are activated (McCroskery et al., 2005) . Additionally, higher levels of myostatin are observed during immobilization, resulting in suppression of satellite cell activation (Carlson et al., 1999). In vitro studies revealed that myostatin null mice also exhibit greater proliferation and earlier differentiation of satellite cells (Wagner et al., 2005).

Clenbuterol perhaps plays a less direct role in satellite cell activation than myostatin, although it does induce hypertrophy. While clenbuterol directly affects the rate of protein synthesis- as shown by an up regulation in translational machinery (Spurlock et al., 2006), the direct effect on satellite cell activation has not been elucidated. In whole muscle transplants, proliferation of satellite cells occurs sooner with clenbuterol treatment than without treatment (Roberts & McGeachie, 1992). Innervated and denervated muscles treated with clenbuterol exhibit increased activation of satellite cells; however, increases in mitosis are not observed (Maltin & Delday, 1992). Therefore, the effect of clenbuterol on satellite cell activity may be secondary to its' effects on protein synthesis and degradation.

Muscle Fiber Types

Following differentiation, myoblasts fuse to form myotubes with centralized nuclei. Two waves of fusion occur. The first wave gives rise to primary muscle fibers

which are generally slow and oxidative in mature animals. A second wave of fusion gives rise to secondary muscle fibers. These can become either fast or slow muscle fibers in mature animals. These myotubes accumulate myofibrils, the contractile units of mature muscle, and the nuclei are pushed to the periphery of the cell. Muscle fiber types are specialized and vary in their energy metabolism, contractile properties, and functionality (Edstrom & Kugelberg, 1968). Slow twitch (red) fibers utilize oxidative metabolism and are fatigue-resistant. Fast-twitch (white) fibers are more suited to use glycolytic metabolism but are not fatigue-resistant.

Muscle fibers can also be classified by myosin heavy chain (MHC) expression. The predominant protein in muscle fibers is myosin, consisting of four light chains and two heavy chains. The major MHC isoforms determine the contractile properties of a fiber, and they are categorized differently based on their ATPase activity in the head region of the heavy chain (Brooke & Kaiser, 1970). The major skeletal muscle MHC isoforms in mature muscle include MHCI, the slowest isoform, MHCIIb, the fastest, and MHCIIa and MHCIIx, which have intermediate contractibility. Not all species exhibit the same distribution of fiber types and MHC isoforms. Humans, for example, only exhibit three MHC isoforms (MHCI, MHCIIa, and MHCIIb) (Staron, 1997).

Lack of functional myostatin impacts fiber type in skeletal muscle. Cattle with mutations in myostatin express more of fast, glycolytic isoforms (Wegner et al., 2000). Additionally, myostatin null mice exhibit more fast fibers in both slow and fast muscles as well as a greater proportion of fast MHC isoforms (Girgenrath, Song, & Whittemore, 2005). Microarray analysis also suggests an up-regulation in the faster, glycolytic MHC isoforms (Steelman et al., 2006).

Administration of clenbuterol affects the contractile properties and metabolism of muscle fibers as well. In rats, slow to fast muscle fiber type transition occurs in response to treatment with clenbuterol (Ricart-Firinga et al., 2000; Zeman et al., 1988). In addition to altering muscle fiber type in rats, clenbuterol administration alters the MHC isoforms to favor the fast types and as a result induces metabolic adaptations to favor glycolytic metabolism (Rajab et al., 2000).

Increased expression of faster fiber types in hypertrophied muscle may result from differences in hypertrophic capacity of different fiber types. Faster fibers are larger in diameter and have a greater potential to undergo hypertrophy. Conversely, slower fibers, which are more dependent on the diffusion of oxygen for oxidative metabolism, are smaller in size and undergo less hypertrophy. Therefore, changes in fiber type distribution may reflect hypertrophic potential more than direct effects on expression of MHC proteins. This is not surprising as skeletal muscle hypertrophy preferentially occurs in the larger, type 2 muscle fibers in response to myostatin inactivation (Wegner et al., 2000) and clenbuterol administration (Kim & Sainz, 1992).

Objectives

Both myostatin and clenbuterol are powerful modulators of muscle growth. The lack of functional myostatin and clenbuterol treatment are similar in that they both increase muscle mass and alter muscle fiber types. The same pathways have been implicated for both. However, they are different because myostatin affects both prenatal development and postnatal growth whereas postnatal clenbuterol treatment only affects postnatal growth. Therefore, the objective of the following studies was to identify similar

and disparate pathways leading to muscle hypertrophy in myostatin null and wild type mice treated with clenbuterol.

Techniques for Identifying Pathways of Muscle Hypertrophy

Microarray

Recent scientific advances, such as the sequencing of full genomes, have created a tremendous opportunity for researchers. With these advances and other discoveries, tools for studying thousands of genes at once have become available. One such example is DNA microarrays. The concept of microarrays stems from basic concepts of gene expression. While every cell in an organism possesses the same DNA, cells differ in the timing, intensity, and identity of genes they express. Gene expression is measured in the amount of messenger RNA (mRNA) produced for a particular gene. Techniques such as Northern blots or RT-PCR quantify expression of one gene at a time. Microarrays allow examination of far more genes- up to the whole genome- at once and have been shown to elicit similar results as Northern blots (Taniguchi et al, 2001). In addition to examining thousands of genes in parallel, microarrays compare gene expression profiles between two or more mRNA samples. However, while microarrays provide insight into gene expression, protein expression, enzyme kinetics and other means must also be used to determine whether or not differences in transcription translate into physiological differences.

Two different types of microarrays exist: complementary DNA (cDNA) microarrays and oligonucleotide microarrays. In cDNA microarrays, also known as spotted arrays, samples of cDNA, oligonucleotides, or other PCR products are synthesized prior to being affixed, or "spotted" on the microscope slide (Schena et al.,

1995). Conversely, oligonucleotide arrays are composed of short complementary sequences of specific oligonucleotides that are synthesized directly on the microscope slides (Lockhart et al., 1996). Most microarrays utilize coated microscope slides with spots placed on the surface either through robotic spotting (Schena et al., 1995) or by using modified inkjet technology (Hughes et al., 2001). Microarrays can contain an entire genome or contain only specific genes of interest to a particular research field. For a genome-wide microarray, the genome must be sequenced and annotated. On the array, every gene is represented by a "spot" and this spot contains multiple copies of a DNA sequence unique to that particular gene.

The procedure to perform a microarray analysis contains a series of basic steps including isolation of mRNA, production of labeled cDNA, hybridization of cDNA to the array and scanning to determine expression. Total RNA, containing mRNA and other forms, is isolated from a tissue of interest. Isolation of mRNA molecules away from other types of RNA is accomplished by binding the poly-adenine tail of the mRNA with buffers or columns. A copy of cDNA is produced from the mRNA by reverse transcription. Using labeled nucleotides in the reverse transcriptase reaction making cDNA from mRNA results in a pool of labeled cDNA and facilitates comparing gene expression from two different samples. Cy3, fluorescent at 570 nm and greenish in color, and Cy5, fluorescent at 670 nm and reddish in color, are the two most commonly used dyes. In the hybridization process, single-stranded cDNA binds to single-stranded DNA attached to the microarray slide.

After washing away unbound cDNA, microarrays are scanned by lasers to excite the fluorophores and are visualized. More intense fluorescence corresponds to more

binding of cDNA at a particular spot and therefore, corresponds to increased expression of that particular gene in the tissue of interest. Microarray scanners generally scan green (Cy3), red (Cy5) and yellow (the overlap of the two dyes), allowing for expression of genes to be compared between two samples. Once the microarray has been scanned, the relative intensities of each fluorophore are used in ratio-based analysis to identify up-regulated and down-regulated genes (Tang et al., 2007).

Various uses for microarray technology exist. Because microarrays analyze thousands of genes simultaneously, gene expression differences can be determined between different tissues, time points, or treatments (Schulze & Downward, 2001). Microarrays are effective for studying small-sized samples and produce copious results quickly. However, with all of these advantages also come drawbacks. While microarrays generate large amounts of data, the data are simply lists of single genes which are up or down-regulated. Additionally, microarray results must be validated with other applications. Oftentimes validation may be a simple comparison of current results with past literature published on a subject (Chuaqui et al., 2002). Results may also be validated by laboratory techniques such as Western blots to determine actual protein concentrations, or Northern blots and quantitative RT-PCR to determine mRNA levels (Lockhart & Winzeler, 2000). Enzyme assays can also be utilized to determine if increased transcription results in increased enzyme activity.

In order to accommodate all of the data generated from microarray analysis, the Gene Ontology (GO) annotation was created. Gene annotation clusters single genes into functional groups and pathways. Three separate ontology categories are used: biological process, molecular function, and cellular component. The biological process category

allows researchers to visualize all of the known processes in which a specific gene or group of genes is involved. The molecular function category describes what the gene or gene product does, but not necessarily where or when the event occurs. The cellular component of GO illustrates where in the cell a gene product is active. This system allows researchers to identify relationships between genes of interest as well as define the function of unknown genes (The Gene Ontology Consortium, 2000; 2001).

Real-time quantitative PCR

Another way to examine genes of interest generated from a microarray is by RT-PCR. Unlike conventional PCR, RT-PCR collects data as the PCR process occurs, rather than at the endpoint of the reaction. Researchers use RT-PCR because it quantifies differences in mRNA expression but uses smaller amounts of RNA than Northern blotting (reviewed by Bustin, 2002). This is advantageous when experiments generate only small amounts of RNA such as in cell culture experiments or with samples from small animals.

The RT-PCR procedure uses either a one-step or two-step approach. In the one-step approach, reverse transcription and PCR are both performed in the same reaction tube. In the two step approach, reverse transcription is performed prior to RT-PCR. The one-step approach is quicker, less expensive, and requires less handling of samples reducing pipeting errors and possible contamination. Gene specific primers are used during reverse transcription, however, limit quantification to one gene at a time. The two-step approach uses random hexamer or oligonucleotide-dt primers to amplify all the mRNA present allowing for multiple genes to be investigated simultaneously (reviewed by Wong & Medrano, 2005). Also, two-step converts RNA into cDNA which is easier to

store and less susceptible to degradation than RNA. Studies have shown that while the two approaches are similar in efficiency, the two-step approach may be slightly more sensitive and able to detect genes expressed in lower quantities (Peters, 2004).

During real time reactions using Applied Biosytems Taqman Primer/Probe system, release of a fluorescent molecule is measured (Heid et al., 1996). Probes contain two fluorescent dyes; one which serves as a reporter at the 5' end of the primer and one that serves as a quencher on the 3'end. The close position of the quencher dye greatly reduces the fluorescence of the reporter dye (by fluorescence resonance energy transfer). When the probe anneals to a target sequence, it is cleaved by the 5' exonuclease activity of Taq DNA Polymerase as the primer is extended (Holland et al., 1991). Upon cleavage, the reporter dye emission is no longer transferred to the quencher dye, thus, fluorescence only occurs when new DNA is synthesized from the cDNA template.

The point at which the fluorescence crosses a threshold is known as the number of cycles to threshold (Ct). Fewer cycles are needed to produce a detectable signal when a greater amount of target molecules are present. Therefore a lower Ct value means more mRNA of a target sequence was present while a higher Ct values corresponds to less mRNA produced for a target sequence (Higuchi et al., 1993). The Ct values are then standardized to the Ct of a housekeeper gene, a gene whose expression is stable among treatments. This standardizes between samples for differences in starting cDNA concentrations. Mathematical calculations allow for comparisons between groups or treatments in a fold-change manner. A fold change equal to one indicates no differences in mRNA expression between treatments. Fold changes greater than one indicate up-

regulation of mRNA, and fold changes less than one indicate down-regulation of specific mRNA.

Literature Cited

Amirouche, A., Durieux, A., Banzet, S., Koulmann, N., Bonnefoy, R., Mouret, C., X Bigard, X., Peinnequin, A., and Freyssenet, D. (2009). Down-regulation of Akt/Mammalian target of rapamycin signaling pathway in response to myostatin overexpression in skeletal muscle. *Endocrinology, 150*, 286-294.

Awede, B. L., Thissen, J. P., and Lebacq, J. (2002). Role of IGF-I and IGFBPs in the changes of mass and phenotype induced in rat soleus muscle by clenbuterol. *American Journal of Physiology- Endocrinology and Metabolism, 282*, 31-37.

Bogdanovich, S., Krag, T. O. B., Barton, E. R., Morris, L. D., Whittemore, L. A., Ahima, R. S., and Khurana, T.S. (2002). Functional improvement of dystrophic muscle by myostatin blockade. *Nature A-Z Index, 420*, 418-421.

Brooke, M. H., and Kaiser, K. K. (1970). Muscle fiber types- how many and what kind? *Archives of Neurology, 23*, 369-379.

Bustin, S. (2002). Quantification of mRNA using real-time reverse transcription PCR (RT-PCR): Trends and problems. *Journal of Molecular Endocrinology, 29*, 23-39.

Carlson, C. J., Booth, F. W., and Gordon, S. E. (1999). Skeletal muscle myostatin mRNA expression is fiber-type specific and increases during hindlimb unloading. *American Journal of Physiology- Regulatory, Integrative and Comparative Physiology, 277*, 601-606.

Chelh, I., Meunier, B., Picard, B., Reecy, M., Chevalier, C., Hocquette, J., and Cassar-Malek, I. (2009). Molecular profiles of quadriceps muscle in myostatin-null mice reveal PI3K and apoptotic pathways as myostatin targets. *BMC Genomics, 10*, 196-209.

Chen, J., and Goldhamer, D. (2003). Skeletal muscle stem cells. *Reproductive Biology and Endocrinology, 1*, 101-108.

Chuaqui, R. F., Bonner, R. F., Best, C. J. M., Gillespie, J. W., Flaig, M. J., Hewitt, S. M., Phillips,J. L., Krizman, D. B., Tangrea,M. A., Ahram, M., Linehan,W.M., Knezevic,V., Emmert, B., and Michael, R. (2002). Post-analysis follow-up and validation of microarray experiments. *Nature Genetics, 32*, 509-514.

Clop, A., Marcq, F., Takeda, H., Pirottin, D., Tordoir, X., Bibe, B., Bouix, J., Caiment, F., Elsen, J., Eychenne, F., Larzul, C., Laville, E., Meish, F., Milenkovic, D., Tobin, J., Charlier, C., and Georges, M. (2006). A mutation creating a potential illegitimate microRNA target site in the myostatin gene affects muscularity in sheep. *Nature Genetics, 38*, 813-818.

Cornelison, D. D. W., Olwin, B. B., Rudnicki, M. A., and Wold, B. J. (2000). MyoD−/− satellite cells in single-fiber culture are differentiation defective and MRF4 deficient. *Developmental Biology, 224*, 122-137.

Costelli, P., Garcia-Martinez, C., Llovera, M., Carbo, N., Lopez-Soriano, F., Agell, N., Tessitore, L., Baccino, F.M., and Argiles, J.M. (1995). Muscle protein waste in tumor-bearing rats is effectively antagonized by a beta 2-adrenergic agonist (clenbuterol). role of the ATP-ubiquitin-dependent proteolytic pathway. *Journal of Clinical Investigation, 95*, 2367- 2372.

Edstrom, L., and Kugelberg, E. (1968). Histochemical composition, distribution of fibres and fatiguability of single motor units. anterior tibial muscle of the rat. *Journal of Neurology, Neurosurgery, and Psychiatry, 31*, 424-433.

Girgenrath, S., Song, K., and Whittemore, L. A. (2005). Loss of myostatin expression alters fiber-type distribution and expression of myosin heavy chain isoforms in slow- and fast-type skeletal muscle. *Muscle & Nerve, 31*, 34-40.

Glass, D. J. (2003). Signalling pathways that mediate skeletal muscle hypertrophy and atrophy. *Nature Cell Biology, 5*, 87-90.

Gonzalez-Cadavid, N., Taylor, W. E., Yarasheski, K., Sinha-Hikim, I., Ma, K., Ezzat, S., Shen, R., Lalani, R., Asa, S., Mamita, M., Nair, G., Arver, S., and Bhasin, S. (1998). Organization of the human myostatin gene and expression in healthy men and HIV-infected men with muscle wasting. *Proceedings of the National Academy of Sciences, 95*, 14938-14943.

Grobet, L. (1998). Molecular definition of an allelic series of mutations disrupting the myostatin function and causing double-muscling in cattle. *Mammalian Genome, 9*, 210-213.

Grobet, L., Martin, L. J. R., Poncelet, D., Pirottin, D., Brouwers, B., Riquet, J., Schoeberlein, A., Dunner, S., Ménissier, F., and Massabanda, J. (1997). A deletion in the bovine myostatin gene causes the double-muscled phenotype in cattle. *Nature Genetics, 17*, 71-74.

Heid, C. A., Stevens, J., Livak, K. J., and Williams, P. M. (1996). Real time quantitative PCR. *Genome Research, 6*, 986-994.

Higgins, J. A., Lasslett, Y. V., Bardsley, R. G., and Buttery, P. J. (1988). The relation between dietary restriction or clenbuterol treatment on muscle growth and calpain proteinase and calpastatin activities in lambs. *British Journal of Nutrition, 60*, 645-652.

Higuchi, R., Fockler, C., Dollinger, G., and Watson, R. (1993). Kinetic PCR analysis: Real-time monitoring of DNA amplification reactions. *Biotechnology, 11*, 1026-1030.

Hill, J. J., Davies, M. V., Pearson, A. A., Wang, J. H., Hewick, R. M., Wolfman, N. M., and Qiu, Y. (2002). The myostatin propeptide and the follistatin-related gene are inhibitory binding proteins of myostatin in normal serum. *Journal of Biological Chemistry, 277*, 40735-40741.

Hinkle, R. T., Hodge, K. M. B., Cody, D. B., Sheldon, R. J., Kobilka, B. K., and Isfort, R. J. (2002). Skeletal muscle hypertrophy and anti-atrophy effects of clenbuterol are mediated by the β2-adrenergic receptor. *Muscle & Nerve, 25*, 729-734.

Holland, P. M., Abramson, R. D., Watson, R., and Gelfand, D. H. (1991). Detection of specific polymerase chain reaction product by utilizing the 5'----3' exonuclease activity of thermus aquaticus DNA polymerase. *Proceedings of the National Academy of Sciences, 88*, 7276-7280.

Hughes, T. R., Mao, M., Jones, A. R., Burchard, J., Marton, M. J., Shannon, K. W., Lefkowitz, S. M., Ziman, M., Schelter, J. M., Meyer, M. R., Kobayashi, S., Davis, C., Dai, H., He,Y. D., Stephaniants, S. B., Cavet, G., Walker, W. L., West, A., Coffey, E., Shoemaker, D. D., Stoughton, R., Blanchard, A. P., Friend, S. H., and Linsley, P. S. (2001). Expression profiling using microarrays fabricated by an ink-jet oligonucleotide synthesizer. *Nature Biotechnology, 19*, 342-347.

Jones, J. I., and Clemmons, D. R. (1995). Insulin-like growth factors and their binding proteins: Biological actions. *Endocrine Reviews, 16*, 3-34.

Kim, Y. S., and Sainz, R. D. (1992). Beta-adrenergic agonists and hypertrophy of skeletal muscles. *Life Sciences, 50*, 397-407.

Kline, W. O., Panaro, F. J., Yang, H., and Bodine, S. C. (2007). Rapamycin inhibits the growth and muscle-sparing effects of clenbuterol. *Journal of Applied Physiology, 102*, 740-747.

Kuang, S., Kuroda, K., Le Grand, F., and Rudnicki, M. A. (2007). Asymmetric self-renewal and commitment of satellite stem cells in muscle. *Cell, 129*, 999-1010.

Langley, B., Thomas, M., Bishop, A., Sharma, M., Gilmour, S., and Kambadur, R. (2002). Myostatin inhibits myoblast differentiation by down-regulating MyoD expression. *Journal of Biological Chemistry, 277*, 49831-49840.

Lockhart, D. J., Dong, H., Byrne, M. C., Follettie, M. T., Gallo, M. V., Chee, M. S., Mittmann, M., Wang, C., Kobayashi, M., Norton, H., and Brown, E. L. (1996). Expression monitoring by hybridization to high-density oligonucleotide arrays. *Nature Biotechnology, 14*, 1675-1680.

Lockhart, D. J., and Winzeler, E. A. (2000). Genomics, gene expression and DNA arrays. *Nature, 405*, 827-836.

Maltin, C., Hay, S., Delday, M., Smith, F., Lobley, G., and Reeds, P. (1987). Clenbuterol, a beta agonist, induces growth in innervated and denervated rat soleus muscle via apparently different mechanisms. *Bioscience Reports, 7*, 525-532.

Maltin, C. A., and Delday, M. I. (1992). Satellite cells in innervated and denervated muscles treated with clenbuterol. *Muscle & Nerve, 15*, 919-925.

Matsumoto, T., Akutsu, S., Wakana, N., Morito, M., Shimada, A., and Yamane, A. (2006). The expressions of insulin-like growth factors, their receptors, and binding proteins are related to the mechanism regulating masseter muscle mass in the rat. *Archives of Oral Biology, 51*, 603-611.

Mauro, A. (1961). Satellite cell of skeletal muscle fibers. *Journal of Cell Biology, 9*, 493-495.

McCroskery, S., Thomas, M., Maxwell, L., Sharma, M., and Kambadur, R. (2003). Myostatin negatively regulates satellite cell activation and self-renewal. *Journal of Cell Biology, 162*, 1135-1147.

McFarlane, C., Plummer, E., Thomas, M., Hennebry, A., Ashby, M., Ling, N., Smith, H., Sharma, M., and Kambadur, R. (2006). Myostatin induces cachexia by activating the ubiquitin proteolytic system through an NF-kappaB-independent, FoxO1-dependent mechanism. *Journal of Cellular Physiology, 209*, 501-514.

McKinnell, I. W., Parise, G., and Rudnicki, M. A. (2005). Muscle stem cells and regenerative myogenesis. In *Current Topics in Developmental Biology* (113-130) Gerald P. Schatten (Editor) Academic Press.

McPherron, A. C., and Lee, S. J. (1997). Double muscling in cattle due to mutations in the myostatin gene. *Proceedings of the National Academy of Sciences, 94*, 12457-12461.

McPherron, A. C., Lawler, A. M., and Lee, S. J. (1997). Regulation of skeletal muscle mass in mice by a new TGF-beta superfamily member. *Nature, 387*, 83-90.

Mersmann, H. (1998). Overview of the effects of beta-adrenergic receptor agonists on animal growth including mechanisms of action. *Journal of Animal Science, 76*, 160-172.

Mosher, D. S., Quignon, P., Bustamante, C. D., Sutter, N. B., Mellersh, C. S., Parker, H. G., and Ostrander, E. A. (2007). A mutation in the myostatin gene increases muscle mass and enhances racing performance in heterozygote dogs. *PLoS Genetics, 3*, 779-786.

Navegantes, L. C. C., Resano, N. M. Z., Migliorini, R. H., and Kettelhut, I. C. (2001). Catecholamines inhibit Ca2+-dependent proteolysis in rat skeletal muscle through β2-adrenoceptors and cAMP. *American Journal of Physiology- Endocrinology and Metabolism, 281*, E449-E454.

Oldham, J. M., Martyn, J. A. K., Sharma, M., Jeanplong, F., Kambadur, R., and Bass, J. J. (2001). Molecular expression of myostatin and MyoD is greater in double-muscled than normal-muscled cattle fetuses. *American Journal of Physiology-Regulatory, Integrative and Comparative Physiology, 280*, R1488-R1493.

Rajab, P., Fox, J., Riaz, S., Tomlinson, D., Ball, D., and Greenhaff, P. (2000). Skeletal muscle myosin heavy chain isoforms and energy metabolism after clenbuterol treatment in the rat. *American Journal of Physiology- Regulatory, Integrative and Comparative Physiology, 279*, 1076-1081.

Ricart-Firinga, C., Stevens, L., Canu, M. H., Nemirovskaya, T. L., and Mounier, Y. (2000). Effects of β2-agonist clenbuterol on biochemical and contractile properties of unloaded soleus fibers of rat. *American Journal of Physiology- Cell Physiology, 278*, 582-588.

Ricks, C., Baker, P., and Dalrymple, R. (1984). Use of repartitioning agents to improve performance and body composition of meat animals. *Reciprocal Meat Conference Proceedings, 37*, 5-11.

Rios, R., Carneiro, I., Arce, V. M., and Devesa, J. (2002). Myostatin is an inhibitor of myogenic differentiation. *American Journal of Physiology- Cell Physiology, 282*, C993-C999.

Ríos, R., Carneiro, I., Arce, V. M., and Devesa, J. (2001). Myostatin regulates cell survival during C2C12 myogenesis. *Biochemical and Biophysical Research Communications, 280*, 561-566.

Roberts, P., & McGeachie, J. (1992). The effects of clenbuterol on satellite cell activation and the regeneration of skeletal muscle: An autoradiographic and morphometric study of whole muscle transplants in mice. *Journal of Anatomy, 180*, 57-65.

Schena, M., Shalon, D., Davis, R., and Brown, P. (1995). Quantitative monitoring of gene expression patterns with a complementary DNA microarray. *Science, 270*, 467-470.

Schmidt, P., Holsboer, F., and Spengler, D. (2001). β2-adrenergic receptors potentiate glucocorticoid receptor transactivation via G protein β γ-subunits and the phosphoinositide 3-kinase pathway. *Molecular Endocrinology, 15*, 553-564.

Schuelke, M., Wagner, K. R., Stolz, L. E., Hubner, C., Riebel, T., Komen, W., Braun, T., Tobin, J. F., and Lee, S. J. (2004). Myostatin mutation associated with gross muscle hypertrophy in a child. *New England Journal of Medicine, 350*, 2682-2688.

Schulze, A., and Downward, J. (2001). Navigating gene expression using microarrays- A technology review. *Nature Cell Biology, 3*, E190- E195.

Sherr, C. J., and Roberts, J. M. (1999). CDK inhibitors: Positive and negative regulators of G1-phase progression. *Genes & Development, 13*, 1501-1512.

Sneddon, A. A., Delday, M. I., Steven, J., and Maltin, C. A. (2001). Elevated IGF-II mRNA and phosphorylation of 4E-BP1 and p70S6k in muscle showing clenbuterol-induced anabolism. *American Journal of Physiology - Endocrinology and Metabolism, 281*, E676-E682.

Snow, M. H. (1977). The effects of aging on satellite cells in skeletal muscles of mice and rats. *Cell and Tissue Research, 185*, 399-408.

Spurlock, D. M., McDaneld, T. G., and McIntyre, L. M. (2006). Changes in skeletal muscle gene expression following clenbuterol administration. *BMC Genomics, 7*, 320-335.

Staron, R. S. (1997). Human skeletal muscle fiber types: Delineation, development, and distribution. *Canadian Journal of Applied Physiology, 22*, 307-327.

Steelman, C. A., Recknor, J. C., Nettleton, D., and Reecy, J. M. (2006). Transcriptional profiling of myostatin-knockout mice implicates Wnt signaling in postnatal skeletal muscle growth and hypertrophy. *The FASEB Journal, 20*, 580-582.

Tang, T., Francois, N., Glatigny, A., Agier, N., Mucchielli, M., Aggerbeck, L., and Delacroix, H. (2007). Expression ratio evaluation in two-colour microarray experiments is significantly improved by correcting image misalignment. *Bioinformatics, 23*, 2686-2691.

Taniguchi, M., Miura, K., Iwao, H., and Yamanaka, S. (2001). Quantitative assessment of DNA Microarrays—Comparison with northern blot analyses. *Genomics, 71*, 34-39.

Taylor, W. E., Bhasin, S., Artaza, J., Byhower, F., Azam, M., Willard, D. H., Kull, F.C., and Gonzalez-Cadavid, N. (2001). Myostatin inhibits cell proliferation and protein synthesis in C2C12 muscle cells. *American Journal of Physiology- Endocrinology and Metabolism, 280*, E221-E228.

The Gene Ontology Consortium. (2000). Gene Ontology: Tool for the unification of biology. *Nature Genetics, 25*, 25-29.

The Gene Ontology Consortium (2001). Creating the Gene Ontology resource: Design and implementation. *Genome Research, 11*, 1425-1433.

Thomas, M., Langley, B., Berry, C., Sharma, M., Kirk, S., Bass, J., and Kambadur, R. (2000). Myostatin, a negative regulator of muscle growth, functions by inhibiting myoblast proliferation. *Journal of Biological Chemistry, 275*, 40235-40243.

Wagner, K. R., Liu, X., Chang, X., and Allen, R. E. (2005). Muscle regeneration in the prolonged absence of myostatin. *Proceedings of the National Academy of Sciences, 102*, 2519-2524.

Wegner, J., Albrecht, E., Fiedler, I., Teuscher, F., Papstein, H. J., and Ender, K. (2000). Growth- and breed-related changes of muscle fiber characteristics in cattle. *Journal of Animal Science, 78*, 1485-1496.

Williams, B., and Ordahl, C. (1994). Pax-3 expression in segmental mesoderm marks early stages in myogenic cell specification. *Development, 120*, 785-796.

Williams, R. S., Caron, M. G., and Daniel, K. (1984). Skeletal muscle beta-adrenergic receptors: Variations due to fiber type and training. *American Journal of Physiology - Endocrinology and Metabolism, 246*, E160-E167.

Wong, M. L., and Medrano, J. F. (2005). Real-time PCR for mRNA quantitation. *BioTechniques, 39*, 75-85.

Yang, J., Ratovitski, T., Brady, J. P., Solomon, M. B., Wells, K. D., and Wall, R. J. (2001). Expression of myostatin pro domain results in muscular transgenic mice. *Molecular Reproduction and Development, 60*, 351-61.

Yimlamai, T., Dodd, S. L., Borst, S. E., and Park, S. (2005). Clenbuterol induces muscle-specific attenuation of atrophy through effects on the ubiquitin-proteasome pathway. *Journal of Applied Physiology, 99*, 71-80.

Zeman, R., Ludemann, R., and Etlinger, J. (1987). Clenbuterol, a beta 2-agonist, retards atrophy in denervated muscles. *American Journal of Physiology- Endocrinology and Metabolism, 252*, 152-155.

Zeman, R., Ludemann, R., Easton, T., and Etlinger, J. (1988). Slow to fast alterations in skeletal muscle fibers caused by clenbuterol, a beta 2-receptor agonist. *American Journal of Physiology- Endocrinology and Metabolism, 254*, 726-732.

Zeman, R. J., Peng, H., Danon, M. J., and Etlinger, J. D. (2000). Clenbuterol reduces degeneration of exercised or aged dystrophic (mdx) muscle. *Muscle & Nerve, 23*, 521-528.

Zimmers, T. A., Davies, M. V., Koniaris, L. G., Haynes, P., Esquela, A. F., Tomkinson, K. N., McPherron, A.C., Wolfman, N. M., and Lee, S. J. (2002). Induction of cachexia in mice by systemically administered myostatin. *Science, 296*, 1486-1488.

CHAPTER 2

GENE EXPRESSION PROFILING OF WILD TYPE AND MYOSTATIN NULL MICE TREATED WITH CLENBUTEROL

Abstract

Increasing muscle growth is beneficial to the meat animal industry and for biomedical research. Altering myostatin function and administration of β-adrenergic agonists, such as clenbuterol, enhances muscle growth. However, it is unclear whether the mechanisms of these effects converge in single pathway. Previous work demonstrated that myostatin null mice (MKO) did respond to clenbuterol with increased body and muscle weights suggesting disparate mechanisms for each effect. We examined gene expression profiles of these mice to identify downstream targets of myostatin null- and clenbuterol-induced skeletal muscle hypertrophy. Microarray analysis was not successful at identifying gene expression differences between clenbuterol-treated and control mice. Differences in gene expression between the MKO mice and wild type (WT) mice were observed including changes in genes related to amino acid and derivative metabolism, development, muscle contraction, transport, and Wnt receptor signaling. These processes are linked to skeletal muscle hypertrophy and may provide interesting targets for future investigation.

Introduction

Altering muscle growth has many applications for animal production and human health. Skeletal muscle is important for locomotion and metabolism, and because muscle is converted to meat postmortem, it is highly targeted in animal research studies. Muscles grow by one of three mechanisms: by hyperplasia (increased cell number), by

hypertrophy (increased cell size), or by increasing the amount of material between cells. Muscle growth, therefore, can be manipulated by various methods.

One approach to increasing muscle growth is by altering functionality of myostatin, a negative regulator of muscle growth. In cattle, natural mutations in the myostatin gene cause hyperplasia and increased muscle mass (Grobet et al., 1997; Grobet et al., 1998; Kambadur et al, 1997; McPherron et al., 1997). The function of myostatin has been highly conserved across species with mutations also causing hyper-muscularity in dogs (Mosher et al., 2007), sheep (Clop et al., 2006), and humans (Schuelke et al., 2004). In addition to these natural mutations, transgenic mice lacking functional myostatin exhibit twice the amount of muscle as normal wild type mice as a result of hyperplasia and hypertrophy (McPherron et al., 1997). These mice provide valuable insight into the study of muscle growth and development.

Mechanistically, myostatin inhibits myoblast cell proliferation by increasing the cell cycle inhibitor, p21, thus maintaining myoblasts in G_1 phase of the cell cycle (Thomas et al., 2000, Taylor et al., 2001). Myostatin also reduces myoblast differentiation by inhibiting MyoD expression and other components necessary for differentiation (Langley et al., 2002, Rios et al., 2002, Joulia et al., 2003). In the absence of myostatin, myoblasts are more free to proliferate and differentiate, leading to prenatal hyperplasia (McPherron and Lee, 1997). In the adult animal, myostatin regulates satellite cells (McCroskery et al., 2003) leading to increased satellite cell activity in animals lacking myostatin. Additionally, animals without myostatin exhibit increased expression of fast myosin heavy chain (MHC) isoforms (Girgenrath et al., 2005).

A second method for increasing muscle mass in animals involves the use of β-adrenergic agonists (BAA). Numerous species of animals administered BAA exhibit increased muscle mass including cattle, chickens, pigs, sheep, and mice (reviewed by Ricks, 1984). One such BAA is clenbuterol which exerts its effect by increasing levels of the second messenger, cyclic adenosine monophosphate, activating protein kinase A. This activates several downstream components necessary for increased muscle growth. While the exact mechanism of clenbuterol action is still unclear, administration of this BAA increases protein synthesis (Emery et al, 1984; Claeys et al, 1989) and decreases protein degradation (Maclennan and Edwards, 1989; Anderson, 1991). Clenbuterol also induces a fiber type transformation- favoring faster, more glycolytic fibers (Zeman et al., 1988). While animals administered clenbuterol share similar qualities to animals with myostatin null mutations, exact mechanisms of action for both remain unclear.

Previous work in our lab demonstrated that myostatin null mice (MKO) respond to clenbuterol with increased body and muscle weights (Dilger at al., 2009). In order to determine if this anabolic response resulted from similar or disparate mechanisms, gene expression profiles of myostatin null mice treated with clenbuterol were compared with wild type mice treated with clenbuterol. This approach has previously been used in MKO mice (Steelman et al., 2006) and in wild type mice treated with clenbuterol (Spurlock et al., 2006), but our approach examined the effects of genotype and treatment simultaneously.

Materials and Methods

Animals

Five-week old male mice were classified based on genotype (wild type (WT); n=32 or myostatin null (MKO); n=24) and were assigned to clenbuterol (20ppm in tap water; Sigma-Aldrich, St. Louis, MO, item # C5423) or control (tap water only) treatments. All mice originated from an internal colony and were genotyped for the myostatin null mutation according to McPherron et al. (1997). Mice were housed individually under a 12/12h light/dark cycle and with free access to pelleted rodent chow (Teklad F6 rodent diet, Harlan, Indianapolis, IN) and water for two weeks. At 7 weeks of age, mice were sacrificed by CO_2 inhalation until cessation of breathing, followed by cervical dislocation. Proximate composition of carcasses and individual muscle weights were used to confirm the effect of the transgene and the effect of clenbuterol administration. Results from these mice have been described elsewhere (Dilger et al., 2009) and are displayed in Table 2.1. The tibialis anterior (TA) muscles from four mice of each genotype and treatment were randomly selected for microarray (n=16).

RNA isolation

Total RNA was isolated from muscle using the Trizol method (Invitrogen). Tissues were disrupted in Trizol with a TissueLyser (Qiagen, Valencia, CA). Isolations were carried out according to the manufacturers' directions. Isolated RNA was quantified by spectrophotometry using a Nanodrop spectrophotometer (Nanodrop, Wilmington, DE). Prior to microarray, RNA quality was determined using a 2100 Bioanalyzer (Agilent, Palo Alto, CA).

Microarray procedure

Mouse Exonic Evidence Based Oligonucleotide (MEEBO) Array (Invitrogen) contains 38,467 70-mer 5' amino-modified oligonucleotide probes representing almost 25,000 genes. The MEEBO array includes: 35,302 probes targeting mouse genes, 97 negative control probes, 1,152 positive control probes, and 1,916 doped control probes. All MEEBO slides were printed on Corning UltraGaps slides using a GeneMachines Omnigrid 100 microarray printer in the University of Illinois Functional Genomics Laboratory.

Total RNA from each TA sample was labeled using the Agilent Two Color QuickAmp Labeling Kit (Santa Clara, CA) according to the manufacturer's protocol. In short, 1 μg of each sample was reverse transcribed using a poly-dt promoter primer to create double stranded cDNA. Antisense cRNA was then generated *in vitro* using T7 RNA polymerase which simultaneously amplifies the target sample and incorporates cyanine 3 (Cy3)-cytidine triphosphate (CTP) or cyanine 5 (Cy5)-CTP. To avoid dye bias, the experiments were performed using a loop design with dye swap of Cy3 and Cy5 (Figure 2.1). Samples were cleaned using a Qiagen RNAeasy column (Valencia, CA) and total synthesis and label incorporation was checked on a NanoDrop spectrophotometer. Labeled probe was fragmented and suspended in Agilent hybridization buffer. Slides were prehybridized with buffer containing: 20% Formamide, 5X Denhardts, 6X SSC, 0.1% SDS, 25μg/ml tRNA and hybridized using a Biomicro Maui Mixer hybridization chamber. Following wash, slides were scanned on an Axon 4000B and image analysis carried out using the Axon GenePix Pro 6.1 Image Analysis software.

Statistical analysis

Microarray analysis was performed by a Functional Genomics Bioinformatics Specialist in the W.M. Keck Center for Comparative and Functional Genomics at the University of Illinois. Quality control assessment, data pre-processing, and statistical analysis were performed using the limma (Smyth et al., 2005) package from the Bioconductor project (Gentleman et al, 2004). Spots that were manually flagged as "bad" due to dust specks, scratches, etc. were removed. Background correction was not done because the background was low and even on all the arrays. Within-array normalization for the red and green channels was performed using loess (averaging ratios from dye-swapped hybridizations) on each print-tip group, and between-array normalization on the M values ($\log_2 \frac{\text{Red}}{\text{Green}}$) was done using the scale method (Smyth and Speed, 2003).

A mixed linear model equivalent to a 2x2 factorial ANOVA (genotype by clenbuterol treatment) was fit on the M-values, and an empirical Bayes correction was employed to improve power and decrease false positives when sample sizes are small (Smyth et al., 2004). Contrasts were pulled from the model to test for the main effects (genotype and clenbuterol treatment), the interaction, and four pair-wise comparisons between various genotype x treatment groups. To correct for multiple hypothesis testing within each contrast, the raw *P*-values were adjusted using the False Discovery Rate (FDR) method (Benjamini and Hochberg, 1995). The effect of clenbuterol treatment was not significant and was therefore not included in subsequent analysis.

Gene Ontology Tree Machine (GOTM), a web-based tool for data analysis and data visualization for sets of genes, was used to categorize genes identified as genes of interest to this study (*bioinfo.vanderbilt.edu/gotm/)*. Using a background list of genes

supplied by the user, GOTM estimates the expected number of genes to fall into each GO category by chance. A given GO category is considered enriched ($P<0.01$), or significant, when the observed number of altered genes exceeds the number of expected genes for that GO category (Zhang et al, 2004).

Results and Discussion

Microarray

Microarray analysis identified 14,604 genes as expressed across all arrays, and only these genes were included in subsequent analysis. The effect of clenbuterol on gene expression was minimal, as were the results of specific contrasts of clenbuterol treated and untreated mice. Only four genes were differentially expressed based on the main effect of clenbuterol treatment (FDR-adjusted $P\leq0.10$). Also, only two genes were differentially expressed in clenbuterol-treated WT mice compared with control WT mice and in clenbuterol-treated MKO mice compared with control MKO mice (FDR-adjusted $P\leq0.10$). Furthermore, there was no significant interaction of genotype and treatment with regards to gene expression as detected by microarray.

While a physiological response to clenbuterol was apparent in treated mice (increased body and muscle weights shown in Table 2.1), no significant changes in gene expression were detected. These results conflict with previous microarray data (Spurlock, 2006) which identified many differentially expressed genes when comparing mice treated with clenbuterol to control mice. However, between our study and the one previously published, there were differences in animal age, clenbuterol dosage and mode of administration, and the microarray platform which all could have contributed to differences between the two studies. Also, treatment duration was longer in our study

which may have diluted some of the gene expression effects. Furthermore, it is possible that changes in gene expression were too small for the assay to detect due to our limited sample size.

The effect of genotype on gene expression, however, was apparent from both the specific contrast of MKO and WT control mice and the overall main effect of genotype. The comparison of MKO control mice with WT control mice identified 277 genes as significant (FDR-adjusted *P*-value ≤ 0.10); however, with a more stringent FDR adjusted *P*-value ≤ 0.05, only 6 genes were differentially expressed. Examining the main effect of genotype, 2428**,** 854, and 130 genes were differentially expressed based on FDR-adjusted *P*-values 0.20, 0.10, and 0.05 respectively. These results were similar to previous microarray (Steelman et al, 2006) comparing MKO and WT mice at five weeks of age.

Gene ontology annotation

Gene Ontology Tree Machine (GOTM) was used to annotate genes deemed significant. Gene set for ontology analysis was extended to include all genes with an FDR of 20% or lower to yield a more complete overview; however, genes were limited to those with fold changes ≥1.4 (expressing 40% more of a particular mRNA) or ≤ 0.6 (expressing only 60% of a particular mRNA). Overall, this set included 255 genes (listed in Appendix). This set was analyzed by GOTM and referenced against the 14,604 genes expressed on the arrays, labeled as background. The distribution of genes in the significant gene list in each Gene Ontology (GO) category was compared to those genes in the background gene list. After the two gene lists were compared, a significance of enrichment (*P*-value) was assigned to each GO category indicating if selected genes were overrepresented in some categories.

Gene Ontology (GO) spans three domains; biological process, molecular function, and cellular component. We focused on the biological process domain. Analysis by GOTM suggested 30 GO categories of enriched gene expression within this domain which were divided into five main groups as shown by Figure 2.1. All of these biological processes contain genes related to skeletal muscle growth and metabolism. All genes from each of the five main categories are shown in Table 2.2-2.5.

The first group consisted of genes related to amino acid and derivative metabolism (Table 2.2). A total of nine genes from this group were altered in MKO mice. This pathway culminated at creatine biosynthesis and metabolism, and therefore creatine biosynthesis was included as a sub-category from this main category. Both enzymes responsible for creatine synthesis, guanidinoacetate methyltransferase (*Gamt)* and glycine amidinotransferase (L-arginine: glycine amidinotransferase) (*Gatm*) were up-regulated in MKO mice compared with WT mice. Therefore, the lack of myostatin may increase creatine synthesis or creatine content in MKO mice.

The second biological process category consisted of genes related to development (Table 2.3). Expression of 41 genes from this group was altered in MKO mice. The role of myostatin in development is to limit muscle growth by inhibiting proliferation of myoblasts (Thomas et al., 2000; Taylor et al., 2001) and differentiation of myoblasts (Langley et al., 2002; Rios et al., 2002; Joulia et al., 2003). Thus, myostatin mutants exhibit hyperplasia (McPherron and Lee, 1997) and the lack of myostatin function in MKO mice would be expected to alter elements of muscle development. Two such genes were up-regulated in the MKO mice compared with the WT mice: homeobox A11 (*Hoxa11*) and sine oculis-related homeobox 2 homolog (Drosophilia) (*Six2*). Previous

research demonstrated that Hoxa11 inhibits MyoD expression in developing limb buds (Yamamoto and Kuroiwa, 2003). Therefore this gene may act similarly to myostatin and decrease proliferation and inhibit differentiation. In a similar manner, Six2 limits expression of myogenin (Spitz et al., 1998) and MyoD (Giordani et al., 2007). The upregulation of these genes may be an adaptation to substitute for the lack of myostatin function.

Another notable gene in this category was the transcription factor forkhead box D3 (*Foxd3*). Embryonic studies with Foxd3 have shown that it is essential for maintaining pluripotent embryonic stem cells (Hanna et al, 2002), and its' increased expression may be related to the expected increase in satellite cells in MKO mice. SRY-box containing gene (*Sox6*), was also up-regulated in MKO mice compared with WT mice. Animals lacking a functional SOX6 protein express predominantly slow MHC isoforms (Hagiwara et al., 2007). Therefore, SOX6 may be related to increasing or maintaining fast fibers, which are increased in MKO mice.

The third group of enriched genes consisted of genes related to muscle contraction (Table 2.4). Expression of nine genes from this group was altered in MKO mice including slow myosin heavy chain isoforms (MHC), *Myhc1* and *Myhc2* corresponding to MHCI and MHCIIa, respectively. Microarray analysis suggested that expression of slower MHC isoforms (I and IIa) was decreased in MKO mice compared with WT mice (FDR-adjusted $P \leq 0.20$), while expression of the fastest MHC isoforms (IIb) was slightly higher (fold change=1.42) in MKO mice compared with WT mice (FDR-adjusted $P \leq 0.20$). Expression of MHCIIx appeared lower in MKO mice compared with WT mice (FC=0.57, data not shown), however the difference was not significant (FDR adjusted

P>0.20). Steelman et al. (2006) found similar down-regulation of slow MHC isoforms with a microarray comparing MKO and WT mice at five weeks of age. Overall, these data would suggest that MKO mice display a faster MHC profile than WT Mice. Alterations in MHC isoforms have previously been illustrated in myostatin mutant animals (Girgenrath et al, 2005) similar to this result.

The fourth group consisted of genes related to transport (Table 2.5). A total of 40 genes from this group were altered in MKO mice. For example, genes involved in fatty acid transport in skeletal muscle, such as fatty acid binding protein 3 (*Fabp3*), Cd36 antigen (*Cd36*), and very low density lipoprotein receptor (*Vldlr*), were down-regulated. Reduced expression of these genes may result in reduced fatty acid transport into muscle of MKO mice. This result may be related to the aforementioned fiber type change in MKO mice. Because myostatin mutant animals have an increased proportion of fast, glycolytic muscle fibers, less fatty acid oxidation may be occurring in these muscles. Therefore, the uptake of fatty acids into the tissue may be decreased, and the elements of fatty acid transport may also be down-regulated.

Other transport genes linked to muscle metabolism were also altered in the MKO mice compared with the WT mice including major urinary proteins (MUPs) which were significantly upregulated in MKO mice compared with WT mice. Recently, administration of recombinant major urinary protein 1 has been shown to enhance insulin signaling via the Akt signaling cascade in skeletal muscle (Hui et al., 2009), however the exact mechanism of mechanisms by which MUPs exert this effect are uncertain. Incorporation of the myostatin null mutation has been shown to reduce insulin resistance

and improve fasting blood glucose in obese lines of mice (McPherron 2002). It is possible that increased expression of MUP would explain this phenomenon.

The fifth group consisted of genes related to Wnt receptor signaling. Four genes from this group were altered in MKO mice. However, the biological process of Wnt receptor signaling was excluded from further analysis because its significance has previously been described (Steelman et al., 2006) who showed that components of the Wnt/Calcium pathway were up-regulated in MKO mice, resulting in increased satellite cell proliferation.

Conclusions

This experiment corroborates with previous microarrays which also demonstrated alteration of genes related to Wnt receptor signaling and muscle contraction (Steelman et al., 2006). Furthermore, several biological processes identified by GO including development and creatine synthesis have been previously linked to myostatin or skeletal muscle hypertrophy.

Other results from the microarray were more surprising. For instance, though a physiological response was observed in clenbuterol-treated MKO and WT mice, there were few changes in gene expression. The original aim of the study was to look for similarities between the two modes of hypertrophy, this, however, was not accomplished. Thus, we cannot conclude from these results whether the modes of action of myostatin null mutation and clenbuterol treatment overlap or are disparate. The additive nature of each effect physiologically would suggest the two mechanisms are separate. To further investigate this matter, it may be beneficial to treat animals for a shorter time period similar to other microarray studies. Also, Spurlock and colleagues (2006) concluded that

the increase in protein synthesis associated with clenbuterol administration may more likely be a result of up-regulation of translational initiators, rather than a sustained up-regulation of gene expression at the transcriptional level. Thus, minimal differences in gene expression would be observed. In the future, we could also re-examine the gene lists more closely and perhaps set less stringent standards for significance.

In summary, this transcriptomic investigation demonstrates that lack of functional myostatin affects the biological processes of development, amino acid and derivative synthesis and metabolism, muscle contraction, transport, and Wnt receptor signaling. Together, these results demonstrate the global effects of altering myostatin activity in mice. While alterations in these biological processes are not surprising, the characterization of many of the genes involved in these processes, particularly skeletal muscle development, is still underway. Further exploration of individual genes and groups of these genes will provide insight into the mechanisms behind skeletal muscle hypertrophy. Therefore, each of these categories should be examined individually to define specific roles of each process and of individual genes within a process. This may help us to better understand the exact mechanisms behind myostatin inhibition of skeletal muscle growth.

Literature Cited

Anderson, P. T., Helferich, W. G., Parkhill, L. C., Merkel, R. A., and Bergen, W. G. (1990). Ractopamine increases total and myofibrillar protein synthesis in cultured rat myotubes. *Journal of Nutrition, 120*, 1677-1683.

Benjamini, Y., and Hochberg, Y. (1995). Controlling the false discovery rate: A practical and powerful approach to multiple testing. *Journal of the Royal Statistical Society Series B, 57,* 289-300.

Dilger, A.C, Gabriel, S.R., Kutzler, L.W., McKeith, F.K., and J. Killefer. (2009) The myostatin null mutation and clenbuterol administration elicit additive effects in mice. Animal (in press).

Claeys, M. C., Mulvaney, D. R., McCarthy, F. D., Gore, M. T., Marple, D. N., and Sartin, J. L. (1989). Skeletal muscle protein synthesis and growth hormone secretion in young lambs treated with clenbuterol. *Journal of Animal Science, 67*, 2245-2254.

Clop, A., Marcq, F., Takeda, H., Pirottin, D., Tordoir, X., Bibe, B., Bouix, J., Caiment, F., Elsen, J., Eychenne, F., Larzul, C., Laville, E., Meish, F., Milenkovic, D., Tobin, J., Charlier, C., and Georges, M. (2006). A mutation creating a potential illegitimate microRNA target site in the myostatin gene affects muscularity in sheep. *Nature Genetics, 38*, 813-818.

Emery, P. W., Rothwell, N. J., Stock, M. J., and Winter, P. D. (1984). Chronic effects of beta 2-adrenergic agonists on body composition and protein synthesis in the rat. *Bioscience Reports, 4*, 83-91.

Gentleman, R., Carey, V., Bates, D., Bolstad, B., Dettling, M., Dudoit, S., Ellis, B., Gautier, L., Ge,Y., Gentry, J., Hornik, K., Hothorn, T., Huber, W., Iacus, S., Irizarry, R., Leisch, F., Li,C., Maechler, M., Rossini, A., Sawitzki, G., Smith, C., Smyth, G., Tierney, L., Yang, J., and Zhang, J. (2004). Bioconductor: Open software development for computational biology and bioinformatics. *Genome Biology, 5*, R80-R96.

Giordani, J., Bajard, L., Demignon, J., Daubas, P., Buckingham, M., and Maire, P. (2007). Six proteins regulate the activation of Myf5 expression in embryonic mouse limbs. *Proceedings of the National Academy of Sciences, 104*, 11310-11315.

Girgenrath, S., Song, K., and Whittemore, L. A. (2005). Loss of myostatin expression alters fiber-type distribution and expression of myosin heavy chain isoforms in slow- and fast-type skeletal muscle. *Muscle and Nerve, 31*, 34-40.

Grobet, L. (1998). Molecular definition of an allelic series of mutations disrupting the myostatin function and causing double-muscling in cattle. *Mammalian Genome, 9*, 210-213.

Grobet, L., Martin, L. J. R., Poncelet, D., Pirottin, D., Brouwers, B., Riquet, J., Schoeberlein, A., Dunner, S., Ménissier, F., and Massabanda, J. (1997). A deletion in the bovine myostatin gene causes the double-muscled phenotype in cattle. *Nature Genetics, 17*, 71-74.

Hagiwara, N., Yeh, M., and Liu, A. (2007). Sox6 is required for normal fiber type differentiation of fetal skeletal muscle in mice. *Developmental Dynamics, 236*, 2062-2076.

Hanna, L. A., Foreman, R. K., Tarasenko, I. A., Kessler, D. S., and Labosky, P. A. (2002). Requirement for Foxd3 in maintaining pluripotent cells of the early mouse embryo. *Genes and Development, 23*, 2650-2661.

Hui, X., Zhu, W., Wang, Y., Lam, K., Zhang, J., Wu, D., Kraegen, E.W., Li, Y., and Xu, A. (2009). Major urinary protein-1 increases energy expenditure and improves glucose intolerance through enhancing mitochondrial function in skeletal muscle of diabetic mice. *Journal of Biological Chemistry, 284*, 14050-14057.

Joulia, D., Bernardi, H., Garandel, V., Rabenoelina, F., Vernus, B., and Cabello, G. (2003). Mechanisms involved in the inhibition of myoblast proliferation and differentiation by myostatin. *Experimental Cell Research, 286*, 263-275.

Kambadur, R., Sharma, M., Smith, T. P., and Bass, J. J. (1997). Mutations in myostatin (GDF8) in double-muscled belgian blue and piedmontese cattle. *Genome Research, 7*, 910-915.

Langley, B., Thomas, M., Bishop, A., Sharma, M., Gilmour, S., and Kambadur, R. (2002). Myostatin inhibits myoblast differentiation by down-regulating MyoD expression. *Journal of Biological Chemistry, 277*, 49831-49840.

MacLennan, P. A., and Edwards, R. H. (1989). Effects of clenbuterol and propranolol on muscle mass. Evidence that clenbuterol stimulates muscle beta-adrenoceptors to induce hypertrophy. *The Biochemical Journal, 264*, 573-579.

McCroskery, S., Thomas, M., Maxwell, L., Sharma, M., and Kambadur, R. (2003). Myostatin negatively regulates satellite cell activation and self-renewal. *Journal of Cell Biology, 162*, 1135-1147.

McPherron, A. C., and Lee, S. J. (1997). Double muscling in cattle due to mutations in the myostatin gene. *Proceedings of the National Academy of Sciences, 94*, 12457-12461.

McPherron, A. C., Lawler, A. M., and Lee, S. J. (1997). Regulation of skeletal muscle mass in mice by a new TGF-beta superfamily member. *Nature, 387*, 83-90.

McPherron, A.C. and Lee, S.-J. (2002) Suppression of body fat accumulation in myostatin-deficient mice. *Journal of Clinical Investigation, 109*, 595-601.

Mosher, D. S., Quignon, P., Bustamante, C. D., Sutter, N. B., Mellersh, C. S., Parker, H. G., and Ostrander, E. A. (2007). A mutation in the myostatin gene increases muscle mass and enhances racing performance in heterozygote dogs. *PLoS Genetics, 3*, 779-786.

Ordway, G. A., and Garry, D. J. (2004). Myoglobin: An essential hemoprotein in striated muscle. *Journal of Experimental Biology, 207*, 3441-3446.

Reeds, P. J., Hay, S. M., Dorwood, P. M., and Palmer, R. M. (2007). Stimulation of muscle growth by clenbuterol: Lack of effect on muscle protein biosynthesis. *British Journal of Nutrition, 56*, 249-258.

Ricks, C., Baker, P., and Dalrymple, R. (1984). Use of repartitioning agents to improve performance and body composition of meat animals. *Reciprocal Meat Conference Proceedings, 37*, 5-11.

Rios, R., Carneiro, I., Arce, V. M., and Devesa, J. (2002). Myostatin is an inhibitor of myogenic differentiation. *American Journal of Physiology - Cell Physiology, 282*, C993-C999.

Schuelke, M., Wagner, K. R., Stolz, L. E., Hubner, C., Riebel, T., Komen, W., Braun, T., Tobin, J. F., and Lee, S. J. (2004). Myostatin mutation associated with gross muscle hypertrophy in a child. *New England Journal of Medicine, 350*, 2682-2688.

Smyth, G. K. (2004). Limma: Linear models for microarray data. In: *Bioinformatics and Computational Biology Solutions using R and Bioconductor* (397-420) Gentleman, R., Carey, V., Dudoit, S., Irizarry, R., and Huber, W. (Editors) Springer, New York.

Smyth, G. K. (2004). Linear models and empirical bayes methods for assessing differential expression in microarray experiments. *Statistical Applications in Genetics and Molecular Biology, 3*, 1-26.

Smyth, G. K., and Speed, T. (2003). Normalization of cDNA microarray data. *Methods, 31*, 265-273.

Spector, A. (1975). Fatty acid binding to plasma albumin. *Journal of Lipid Research, 16*, 165-179.

Spitz, F., Demignon, J., Porteu, A., Kahn, A., Concordet, J., Daegelen, D., and Maire, P. (1998). Expression of myogenin during embryogenesis is controlled by Six/sine oculis homeoproteins through a conserved MEF3 binding site. *Proceedings of the National Academy of Sciences, 95*, 14220-14225.

Spurlock, D. M., McDaneld, T. G., and McIntyre, L. M. (2006). Changes in skeletal muscle gene expression following clenbuterol administration. *BMC Genomics, 7*, 320-335.

Steelman, C. A., Recknor, J. C., Nettleton, D., and Reecy, J. M. (2006). Transcriptional profiling of myostatin-knockout mice implicates Wnt signaling in postnatal skeletal muscle growth and hypertrophy. *The FASEB Journal, 20*, 580-582.

Taylor, W. E., Bhasin, S., Artaza, J., Byhower, F., Azam, M., Willard, D. H., Kull, F.C., and Gonzalez-Cadavid, N. (2001). Myostatin inhibits cell proliferation and protein synthesis in C2C12 muscle cells. *American Journal of Physiology- Endocrinology and Metabolism, 280*, E221-E228.

Thomas, M., Langley, B., Berry, C., Sharma, M., Kirk, S., Bass, J., and Kambadur, R. (2000). Myostatin, a negative regulator of muscle growth, functions by inhibiting myoblast proliferation. *Journal of Biological Chemistry, 275*, 40235-40243.

Yamamoto, M., and Kuroiwa, A. (2003). *Hoxa-11* and *Hoxa-13* are involved in repression of *MyoD* during limb muscle development. *Development Growth and Differentiation, 45*, 485-498.

Zeman, R., Ludemann, R., Easton, T., and Etlinger, J. (1988). Slow to fast alterations in skeletal muscle fibers caused by clenbuterol, a beta 2-receptor agonist. *American Journal of Physiology- Endocrinology and Metabolism, 254*, 726-732.

Zhang, B., Schmoyer, D., Kirov, S., and Snoddy, J. (2004). GOTree machine (GOTM): A web-based platform for interpreting sets of interesting genes using gene ontology hierarchies. *BMC Bioinformatics, 5*, 16-24.

Table 2.1. Effects of genotype (G) and clenbuterol treatment (T) and their interaction (GxT) on body weight, carcass weight and content and tibialis anterior weight of wild type and myostatin null mice[1]

	Wild Type		Myostatin Null		P-value		
	Control	Clenbuterol	Control	Clenbuterol	G	T	GxT
Body weight (g)	22.4 ± 0.53	23.8 ± 0.53	25.9 ± 0.61	27.2 ± 0.59	<0.01	0.02	0.92
Empty carcass weight (g)	8.8 ± 0.29	10 ± 0.29	12.9 ± 0.34	14.1 ± 0.32	<0.01	<0.01	0.99
Empty carcass fat (%)	7.1 ± 0.30	5.4 ± 0.30	4.7 ± 0.38	3.8 ± 0.33	<0.01	<0.01	0.24
Empty carcass protein (%)	20.9 ± 0.22	21.7 ± 0.22	21.5 ± 0.28	22.1 ± 0.24	0.04	0.01	0.69
Tibalis anterior muscle (%) [2]	0.20 ± 0.015	0.23 ± 0.015	0.37± 0.016	0.40 ± 0.016	< 0.01	0.03	0.94

[1] Mice were allowed free access to tap water with 20 ppm clenbuterol (Clenbuterol) or without (Control). Values are lsmeans ± S.E.M.

[2]Expressed as a percentage of body weight.

Figure 2.1. Loop Design utilized for two-color microarray. Samples were hybridized in duplicate using dye swap of Cy3 and Cy5 as demonstrated by the different arrows.

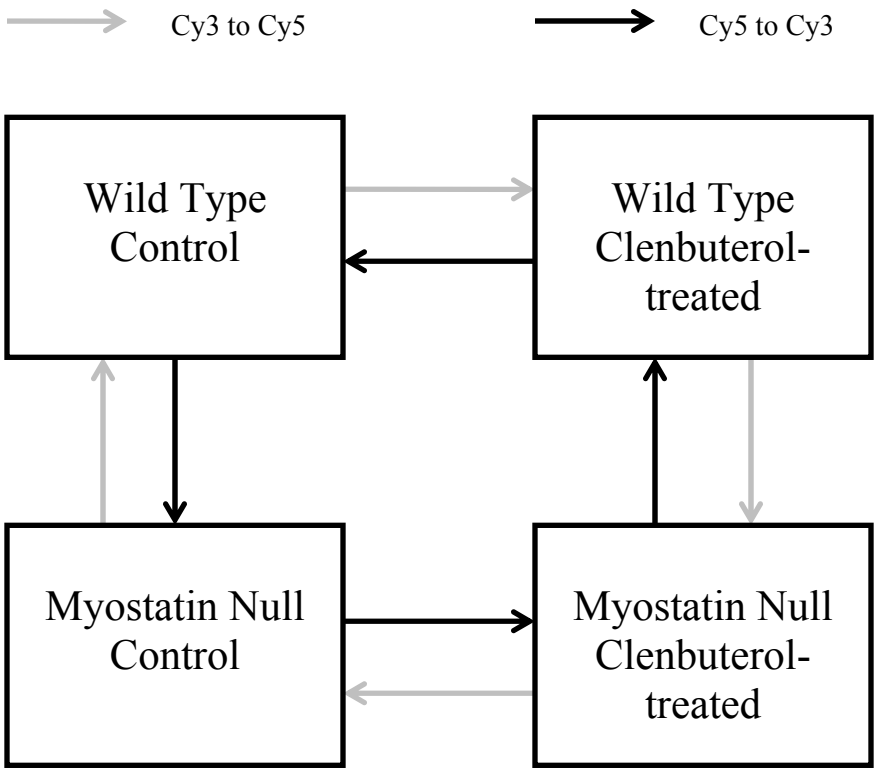


Figure 2.2. Main groups of Biological Processes identified by Gene Ontology Tree Machine analysis. Gene Ontology Tree Machine estimates the expected number of genes to fall into each GO category by chance. A given GO category is considered enriched ($P<0.01$), or significant, when the observed number of altered genes exceeds the number of expected genes for that GO category

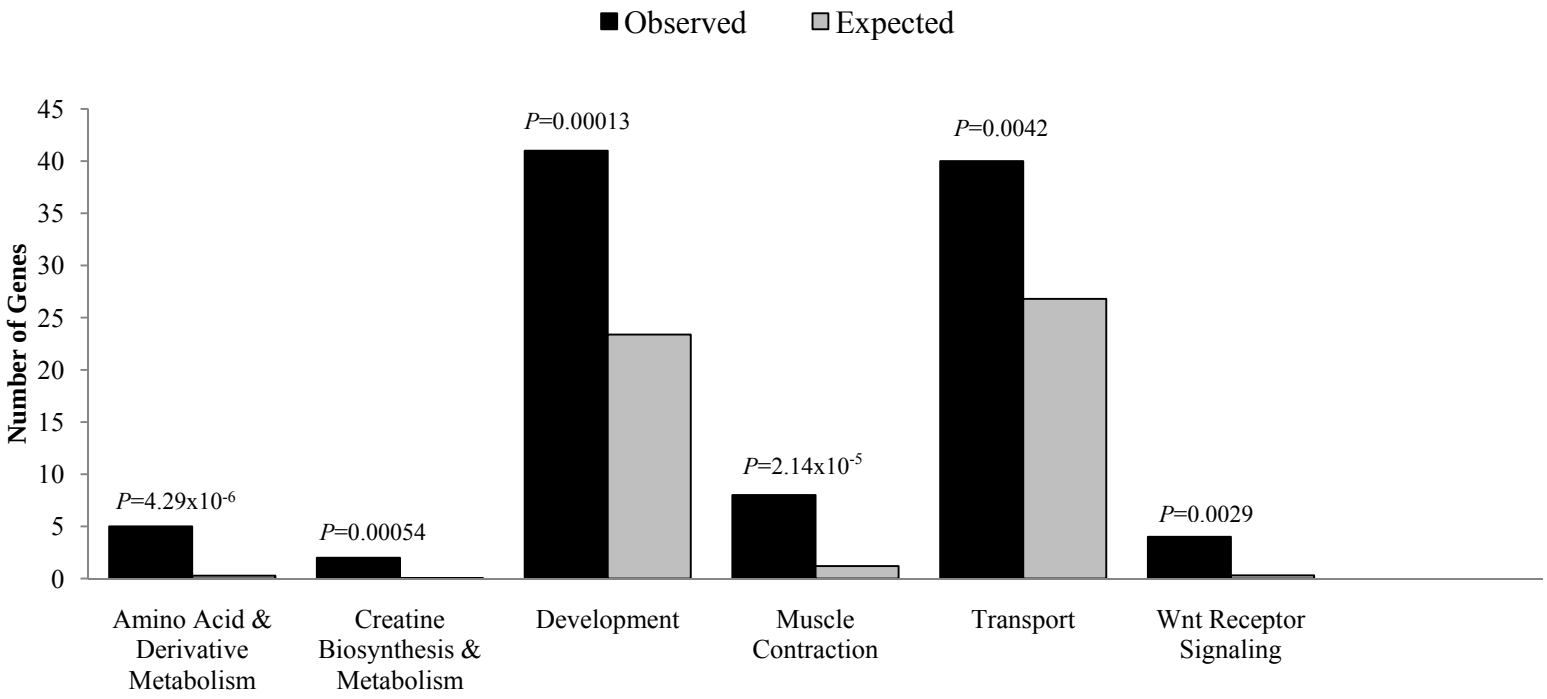


Table 2.2. Genes involved in amino acid and derivative metabolism and creatine biosynthesis and metabolism differentially expressed between myostatin null and wild type mice.

Amino Acid and Derivative Metabolism

Symbol	Gene Name	Fold Change[1]
Amd1	S-adenosylmethionine decarboxylase 1	0.52
Coror2a	coronin, actin binding protein 2A	1.52
Ddc	dopa decarboxylase	1.46
F12a1	coagulation factor XIII, A1 subunit	1.46
Gamt	guanidinoacetate methyltransferase	1.52
Gatm	glycine amidinotransferase (L-arginine:glycine amidinotransferase)	1.66
Nr4a2	nuclear receptor subfamily 4, group A, member 2	1.41
Tph1	tryptophan hydroxylase 1	1.68
Ttr	transthyretin	2.14

Creatine Biosynthesis and Metabolism

Symbol	Gene Name	Fold Change[1]
Gamt	guanidinoacetate methyltransferase	1.52
Gatm	glycine amidinotransferase (L-arginine:glycine amidinotransferase)	1.66

[1]Fold change compares myostatin null to wild type.

Table 2.3 Genes involved in development differentially expressed between myostatin null and wild type mice.

Development

Symbol	Gene Name	Fold Change
Actc1	actin, alpha, cardiac	2.57
Adamst4	a disintegrin-like and metallopeptidase with thrombospondin type 1 motif, 4	1.42
Amd1	S-adenosylmethionine decarboxylase 1	0.52
Ank1	ankyrin 1, erythroid	1.57
Atp6v01a1	ATPase, H+ transporting, lysosomal V0 subunit A1	1.51
Bin1	bridging integrator 1	1.48
Cd28	CD28 antigen	2.22
Chd7	chromodomain helicase DNA binding protein 7	1.41
Csrp3	cysteine and glycine-rich protein 3	0.39
Ctnnbpip1	catenin beta interacting protein 1	1.51
Cxc4	chemokine (C-X-C motif) ligand 4	1.51
Dach2	dachshund 2 (Drosophila)	0.58
Dkk3	dickkopf homolog 3 (Xenopus laevis)	1.78
Emp1	epithelial membrane protein 1	1.63
Esrrg	estrogen-related receptor gamma	0.57
Foxd3	forkhead box D3	1.52
Gab3	growth factor receptor bound protein 2-associated protein 3	1.43
Gamt	guanidinoacetate methyltransferase	1.52
Hoxa11	homeo box A11	1.58
Igf2	insulin-like growth factor 2	2.44
Il15	interleukin 15	0.61
Jun	Jun oncogene	1.40
Kazald1	Kazal-type serine peptidase inhibitor domain 1	1.65
Lgals3	lectin, galactose binding, soluble 3	1.98
Lrp6	low density lipoprotein receptor-related protein 6	1.64
Mafb	v-maf musculoaponeurotic fibrosarcoma oncogene family, protein B	0.54
Mb	myoglobin	0.49
Myh1	myosin, heavy polypeptide 1, skeletal muscle, adult	0.56
Nfic	nuclear factor I/C	1.47
Nov	nephroblastoma overexpressed gene	1.43
Nr4a2	nuclear receptor subfamily 4, group A, member 2	1.41
Nrtn	neurturin	1.42
Pdlim3	PDZ and LIM domain 3	1.46
Pigt	phosphatidylinositol glycan anchor biosynthesis, class T	1.45
Prkg1	protein kinase, cGMP-dependent, type I	0.48
Six2	sine oculis-related homeobox 2 homolog (Drosophilia)	1.42
Sox6	SRY-box containing gene 6	1.54
Spon2	spondin 2, extracellular matrix protein	1.99
Trp63	transformation related protein 63	1.48
Wnt4	wingless-related MMTV integration site 4	1.41

[1]Fold change compares myostatin null to wild type.

Table 2.4 Genes involved in muscle contraction differentially expressed between myostatin null and wild type mice.

Muscle Contraction

Symbol	Gene Name	Fold Change[1]
Actc1	actin, alpha, cardiac	2.57
Actn3	actinin alpha 3	1.68
Atp2a1	ATPase, Ca++ transporting, cardiac muscle, fast twitch 1	1.49
Mybph	myosin binding protein H	2.9
Myh1	myosin, heavy polypeptide 1, skeletal muscle, adult	0.56
Myh3	myosin, heavy polypeptide 3, skeletal muscle, embryonic	0.59
Myh4	myosin, heavy polypeptide 4, skeletal muscle	1.42
Myh8	myosin, heavy polypeptide 8, skeletal muscle, perinatal	2.25
Pde4b	phosphodiesterase 4B, cAMP specific	1.42

[1]Fold change compares myostatin null to wild type.

Table 2.5 Genes involved in Wnt receptor signaling differentially expressed between myostatin null and wild type mice.

Wnt Receptor Signaling

Symbol	Gene Name	Fold Change[1]
Catnbip1	catenin beta interacting protein 1	1.51
Dkk3	dickkopf homolog 3 (Xenopus laevis)	1.78
Lrp6	low density lipoprotein receptor-related protein 6	1.64
Wnt4	wingless-related MMTV integration site 4	1.41

[1]Fold change compares myostatin null to wild type.

Table 2.6 Genes involved in transport differentially expressed between myostatin null and wild type mice.

Transport

Symbol	Gene Name	Fold Change[1]
9530003J23Rik	RIKEN cDNA 9530003J23 gene	0.56
Abca	ATP-binding cassette, sub-family A (ABC1), member 1	0.61
Abra	actin-binding Rho activating protein	1.43
Alb1	albumin 1	4.07
Ambp1	alpha 1 microglobulin/bikunin	1.53
Ank1	ankyrin 1, erythroid	1.57
Ap1m2	adaptor protein complex AP-1, mu 2 subunit	1.45
Atp1b1	ATPase, Na+/K+ transporting, beta 1 polypeptide	0.40
Atp2a1	ATPase, Ca++ transporting, cardiac muscle, fast twitch 1	1.49
Atp6v0a1	ATPase, H+ transporting, lysosomal V0 subunit A1	1.51
BC021785	cDNA sequence BC021785	1.51
Bin1	bridging integrator 1	1.48
C3	complement component 3	0.53
Cd36	CD36 antigen	0.57
Chrna1	cholinergic receptor, nicotinic, alpha polypeptide 1 (muscle)	1.55
Col16a1	procollagen, type XVI, alpha 1	1.41
Col1a1	procollagen, type I, alpha 1	1.67
Emid2	EMI domain containing 2	1.41
Fabp1	fatty acid binding protein 1, liver	2.33
Fabp3	fatty acid binding protein 3, muscle and heart	0.34
Fabp4	fatty acid binding protein 4, adipocyte	0.60
Fndc5	fibronectin type III domain containing 5	0.60
Fth1	ferritin heavy chain 1	1.42
Fxyd6	FXYD domain-containing ion transport regulator 6	0.59
Gatm	glycine amidinotransferase (L-arginine:glycine amidinotransferase)	1.66
Kcnc4	potassium voltage gated channel, Shaw-related subfamily, member 4	1.42
Kif17	kinesin family member 17	1.46
Ktn1	kinectin 1	2.00
Lrp6	low density lipoprotein receptor-related protein 6	1.64
Mb	myoglobin	0.49
Mup1	major urinary protein 1	2.09
Mup2	major urinary protein 2	2.43
Mup3	major urinary protein 3	1.76
Slc16a6	solute carrier family 16 (monocarboxylic acid transporters), member 3	1.54
Sypl2	synaptophysin-like 2	1.55
Tom1l2	target of myb1-like 2 (chicken)	1.45
Ttr	transthyretin	2.14
Tubb6	tubulin, beta 6	1.43
Vldlr	very low density lipoprotein receptor	0.57

[1]Fold change compares myostatin null to wild type.

CHAPTER 3

CHANGES IN GENE EXPRESSION, CREATINE CONTENT AND ENZYME ACTIVITY IN MYOSTATIN NULL MICE AND WILD TYPE MICE

Abstract

Inhibiting myostatin function in animals has provided valuable insight into mechanisms underlying skeletal muscle growth and hypertrophy. However, many of the downstream effects of myostatin remain unclear. Previous microarray analysis by our lab suggested that the myostatin null mutation affects numerous biological processes including development, transport, muscle contraction, and amino acid and derivative metabolism- specifically creatine biosynthesis and metabolism. Real Time PCR (RT-PCR) was employed to validate genes associated with each of these processes in the tibialis anterior (TA), gastrocnemius (GAS), and soleus muscles. Additionally, creatine content and creatine kinase (CK) activity were directly measured in the TA and GAS muscles. Expression of nearly all genes investigated was consistent with microarray analysis, as was expression of myosin heavy chain isoforms. Furthermore, creatine and CK activity were increased in myostatin null mice compared with wild type mice. Therefore this experiment confirms the role of myostatin as a negative regulator of muscle mass and also demonstrates some of the downstream effects of skeletal muscle hypertrophy associated with the myostatin null mutation.

Introduction

Analysis by microarray suggested differences in gene expression between myostatin null (MKO) and wild type (WT) particular to several biological process categories including development, transport, muscle contraction, and amino acid and

derivative metabolism-specifically creatine biosynthesis and metabolism. To confirm these results, genes were selected for validation by Real-Time PCR (Table 3.1). The first three genes, *Meg3*, *Igf2*, and *Il15*, are related to muscle development and growth. *Meg3/Gtl2* is a non-coding RNA whose function is unclear (Miyoshi et al., 2000; Zhou et al., 2007); however, expression of the gene is elevated in sheep with the callipyge mutation (Charlier et al., 2001), suggesting a role for this gene in protein turnover and skeletal muscle hypertrophy. The role of *Igf2*, another maternally imprinted gene, has been highlighted in various growth studies. Gene manipulation studies in mice illustrated that *Igf2* modulates muscle mass during fetal development (DeChiara et al., 1990; Leighton et al., 1995). Additionally, IGF2 partners with IGF1 to stimulate myoblast differentiation (Florini et al., 1991; Pirskanen et al., 2000) and plays a role in satellite cell proliferation (Haugk et al., 1995). Increased mRNA expression of *Igf2* is common in double-muscled cattle breeds as well (Gerrard and Grant, 1994; Listrat et al., 1999). Interleukin 15 (IL15) is a muscle-specific cytokine that has recently been implicated in skeletal muscle hypertrophy (Quinn et al., 2009) and in modulation of fast myosin heavy chain isoforms (Quinn et al., 1995).

The next four genes, cluster of differentiation (*Cd36*), fatty acid binding protein 3 (*Fabp3*), very-low density lipoprotein receptor (*Vldlr*), and lipoprotein lipase (*Lpl*) are involved in fatty acid transport. Overexpression of *Cd36*, also known as fatty acid translocase, enhances fatty acid oxidation in skeletal muscle (Ibrahimi et al., 1999). Conversely, *Cd36* null animals cannot effectively oxidize fatty acids (Coburn et al., 2000). Like *Cd36*, *Fapb3* is involved in fatty acid transport and muscle energy metabolism (Binas and Erol, 2007) and genetic lack of *Fabp3* impairs fatty acid uptake

and oxidation (Binas et al., 1999). Very low density lipoprotein receptor function is not well characterized although mice lacking *Vldlr* exhibit significant reductions in fat mass (Frykman, Brown, Yamamoto, Goldstein, and Herz, 1995). Lipoprotein lipase binds to *Vldlr* (Takahashi et al., 1995) and deficiencies in LPL reduce fat mass-much like *Vldlr* null mice (Weinstock et al., 1997) suggesting a synergistic relationship.

Additionally, microarray analysis and previous work indicated MKO mice displayed a change in fiber type composition (Girgenrath et al., 2005). These changes in fiber type composition are mainly the result of decreased expression of slow myosin heavy chain (MHC) isoforms (Steelman, Recknor, Nettleton, and Reecy, 2006). Because myostatin is preferentially expressed in fast muscle fibers, myostatin mutant animals exhibit primarily fast-twitch fiber hypertrophy (Carlson et al., 1999; Deveaux et al., 2003).

Finally, microarray analysis suggested altered creatine metabolism in MKO mice. Creatine is found in cells with high and fluctuating energy demand such as skeletal muscle and heart (Wyss and Kaddurah-Daouk, 2000), and is synthesized from arginine, glycine, and methionine in two enzyme-catalyzed reactions. The first reaction involves the transfer of an amidino group from arginine to the amino group of glycine. This reaction is catalyzed by L-arginine:glycine amidinotransferase (*Gatm*), and the resulting products are guanidinoacetate (GAA) and ornithine. In the second reaction, GAA is methylated by S-adenosylmethionine (SAM) to produce S-adenosylhomocysteine (SAH) and creatine. This reaction is catalyzed by guanidinoacetate methyltransferase (*Gamt*). Microarray analysis indicated increased expression of both *Gamt* and *Gatm*.

Therefore, the objective of this experiment was to confirm the results of the microarray in a separate replicate of MKO and WT mice. We were interested in extending the result of the microarray which focused on the tibialis anterior muscle to other muscles. Also, we investigated creatine content and activity of creatine kinase directly.

Materials and Methods

Animals

Seven-week old male MKO mice (n=8) from an internal colony and seven-week old male WT mice (n=8) (C57BL/6J, Jackson Laboratories, Ben Harbor, ME) were group housed (4 animals per cage) under a 12/12h light/dark cycle and with free access to pelleted rodent chow (Teklad F6 rodent diet, Harlan, Indianapolis, IN) and water. Mice were sacrificed by CO_2 inhalation until cessation of breathing, followed by cervical dislocation. The following muscles were dissected and weighed from these mice: gastrocnemius (GAS), tibialis anterior (TA), triceps brachii (TB), biceps femoris (BF), and soleus (SOL). Muscle samples were immediately frozen at -80°C and GAS, TA, and SOL muscles were used for RNA extraction and Real-Time PCR (RT-PCR). Because of their small size, SOL muscles from 3 animals were pooled together resulting in only 2 samples of SOL muscle for each genotype.

RNA isolation

Total RNA was isolated from individual TA (n=16) and GAS (n=16) muscles and pooled SOL samples (n=4) using the Trizol method (Invitrogen). Tissues were disrupted in Trizol with a TissueLyser (Qiagen, Valencia, CA). Isolations were carried out

according to the manufacturers' directions. Isolated RNA was quantified by spectrophotometry using a Nanodrop spectrophotometer (Nanodrop, Wilmington, DE).

Real-time PCR

For two-step RT-PCR, cDNA was synthesized from 2µl RNA (0.5µg/µl) using the Quantitect Reverse Transcription Kit (Qiagen, Valencia, CA). cDNA was diluted 1:100 following primer probe validation experiments as recommended by the manufacturer. Real-Time PCR reactions (1µl 1:100 diluted cDNA per reaction) were performed in triplicate on a 7900HT thermal cycler/fluorescence detector (Applied Biosystems, Foster City, CA) using Taqman Universal Master Mix and gene specific primers (Table 3.1) Relative quantification was performed to determine changes in expression of the selected genes in the myostatin null mice compared with the wild type mice. Fold changes in gene expression were determined using the ΔΔCt method (Livak and Schmittgen, 2001) with samples normalized to the level of glyceraldehyde-3-phosphate dehydrogenase *(Gapdh*). Suitability of *Gapdh* as a housekeeper was confirmed by determining that expression of this gene did not differ between genotypes.

Creatine assay

Using manufacturers' recommendations, TA and GAS muscles (30 mg) were homogenized in 1mL of creatine assay buffer containing 0.1% Triton X-100. Homogenates were pelleted by centrifugation (15000 x g for 10 minutes at room temperature) and the supernatant was filtered with a 10K spin filter (BioVision, Mountainview, CA product # 1997) to remove any heavy proteins or enzymes that could interfere with the assay. Samples were diluted 1:100, and creatine content was measured using the Creatine Assay Kit (BioVision, Mountainview, CA). This assay utilizes the

enzymatic conversion of creatine to sarcosine which reacts with an oxidative enzyme to produce peroxide as a byproduct. The peroxide reacts with a probe to produce a colored product detected by spectroscopy at 570 nm after one hour of incubation at 37° C.

Creatine kinase assay

Using manufacturers' recommendations, TA and GAS muscles (30 mg) were homogenized in 1mL of 80mM MES (2-(N-morpholino) ethanesulfonic acid) Buffer pH=6 in a Tissuelyser (Qiagen, Valencia, CA). Homogenates were diluted 1:200 and creatine kinase activity was measured using the EnzyChrom^{TM} Creatine Kinase Assay Kit (BioAssay Systems, Hayward, CA). This assay uses an enzyme-coupled reaction in which creatine phosphate and ADP are converted to creatine and ATP by CK. The generated ATP from this reaction is used by hexokinase to phosphorylate glucose, resulting in the formation of glucose-6-phosphate (G6P). In the presence of G6P dehydrogenase, G6P is oxidized and NADPH is produced. The amount of NADPH produced is proportionate to the CK activity in the sample and is detected by spectroscopy at 340 nm after 10 min and 40 min of incubation at 37° C.

Statistical analysis

All data were analyzed with the MIXED procedure of SAS (Version 9.1; SAS Inst., Inc., Cary, NC, USA). The LSMEANS (least square means) statement was used for means and standard error calculations. For RT-PCR and body weight data, model statement included the main effect of genotype. For creatine and CK activity, the initial model statement included the effect of genotype, muscle, and the genotype x muscle interaction. The muscle x genotype interaction was not significant ($P > 0.05$) so it was removed from the model.

Results and Discussion

Body and muscle weights

Body weight was increased ($P<0.01$) in MKO mice compared with WT mice (Table 3.2). Weights of the triceps brachii, GAS, and TA muscles were increased ($P<0.01$) in MKO mice compared with WT mice with the most pronounced differences between genotypes observed in the triceps brachii and GAS ($P<0.0001$). Muscle weight was increased 24% to 77% in MKO compared with WT mice. Although numerically increased, the biceps femoris of MKO was not statistically different from the WT. Soleus muscle weight, however, from MKO mice (0.013g) and WT mice (0.012g) was not different.

Expression of select genes from microarray analysis

In TA muscle, *Meg3*, *Igf2*, and *Gamt*, were up-regulated ($P<0.05$) in MKO mice compared with WT mice (Figure 3.1A). Conversely, *Lpl* was down-regulated ($P<0.05$) in MKO mice compared with WT mice (Figure 3.1A). Expression of *Fapb3* and *Cd36* was also lower in MKO mice compared to WT mice, but not significant statistically. The expression of *Vldlr* was not consistent with the microarray data presented in Chapter 2 as it was found to be significantly down-regulated by microarray analysis yet up-regulated in RT-PCR analysis ($P<0.05$). Additionally, expression of *Il15* was not altered in TA muscles.

In the GAS muscle, *Meg3*, *Igf2*, and *Gamt* were all up-regulated ($P<0.05$) in the MKO mice compared with the WT mice. Also, *Cd36*, *Fabp3*, and *Lpl* were down-regulated ($P<0.05$) in MKO mice compared with WT mice (Figure 3.1B). In contrast to the result of TA muscle, *Vldlr* expression was lower ($P=0.06$) in the GAS muscle of

MKO mice compared with WT mice and therefore, moves in concert with other fat-transport genes. These results are consistent with previous microarray data from TA muscle with the exception of *Il15*. It was unchanged in the GAS muscle of MKO mice compared with WT mice.

In the SOL muscle, none of the genes examined were found to be statistically different between the MKO mice and the WT mice (Figure 3.1C) perhaps due to the very small sample size for this muscle. Though no genes were statistically different, numerical changes in gene expression observed between MKO mice and WT mice in SOL muscle were similar to the GAS and TA. This included increased *Meg3*, *Igf2*, and *Gam*t expression in MKO mice compared with WT and reduced expression of *Lpl*, *Vldlr*, and *Fabp3*.

Genes from all muscles showed fairly consistent changes in gene expression-aside from *Vldlr* and *Il15*. Microarray analysis showed decreased gene expression of *Vldlr* in TA muscles of MKO mice compared with WT mice. RT-PCR analysis of the TA, however, showed increased gene expression of *Vldlr*. While Weinstock and colleagues (1997) previously suggested a synergistic relationship between *Lpl* and *Vldlr*, *Vldlr* has been shown to function independently of *Lpl* (Tiebel et al., 1999) and this could explain the discrepancy among the related genes. Microarray analysis also showed decreased expression of *Il15* in TA muscle, but RT-PCR analysis showed no significant changes in Il-15 expression between MKO and WT mice in TA and GAS muscle. This could be a result of the cutoff we used for gene annotation purposes (FDR-adjusted p-value ≤ 0.20) in our microarray. Setting significance at 20% means that we accept that 20% of the genes from the list are expected to be false positives, but this was an

acceptable trade off for us to obtain more true positives. This in combination with the borderline fold change of *Il15* (FC=0.61) increases the likelihood that it was not significantly affected by genotype.

Real-time PCR- muscle fiber types

Genes for (MHC) isoforms Myh1, Myh2, Myh7, and Myh4 correspond to proteins MHCI, MHCIIa, MHCIIx, and MHCIIb, respectively and will subsequently be referred to as such. In the TA muscle, MHCI, MHCIIx and MHC IIa were reduced (P <0.06) in MKO mice compared with WT mice (Figure 3.2A). Expression of MHCI, the slowest isoform, was reduced 50% in MKO mice compared with WT mice while expression of MHCIIa and MHCIIx were further reduced. Expression of both intermediate isoforms (MHCIIa and MHCIIx) in MKO mice was less than 10% of WT expression (P< 0.06). Expression of MHCIIb, however, was not altered in MKO mice. These results are consistent with our previous microarray analysis which showed significant down-regulation of MHCI and MHCIIa. In the GAS muscle, only expression of MHCIIa was significantly lower (P<0.01) in MKO mice compared with WT mice (Figure 3.2B). There were no significant differences in MHCI, MHCIIx, or MHCIIb expression between the two genotypes; however, expression of MHCI and MHC2x was numerically lower in MKO mice (P≥0.15).

Overall, the TA and GAS both exhibited reduced gene expression of slow MHC isoforms, rather than an increase in the fastest isoform, MHCIIb. These results, overall, would suggest a shift away from slow isoforms of MHC expression consistent with previous reports (Girgenrath et al., 2005). Steelman and colleagues (2006) also reported similar findings in the pectoralis muscle of MKO mice. Double muscled cattle exhibit

primarily fast-twitch fiber hypertrophy (Wegner et al., 2000; Deveaux et al., 2003). Muscle weight data (Table 3.2) suggested greater hypertrophy in GAS muscles suggesting it possessed more fast fibers. Therefore we expected to see a more pronounced change in MHC isoforms expression in GAS than in TA muscle, but the opposite was true. Therefore, it is unclear which of the two muscles would be considered faster phenotype in MKO mice. To clarify this point, individual muscle fiber size as it relates to muscle fiber type could be examined. Furthermore expression and activity of glycolytic enzymes and oxidative enzymes may provide a clearer picture of fiber type shifts in MKO mice.

In SOL muscle, no significant differences in MHC gene expression were observed between the MKO mice and the WT mice (Figure 3.2C). Expression of both MHCI and MHCIIx was slightly higher in the SOL muscle of MKO mice compared with WT mice but did not reach a level of statistical significance. In the future a larger number of SOL samples should be used. However, given the lack of increase in SOL weight in MKO mice, it is possible that the slow, oxidative soleus is less responsive to the muscle fiber type switching observed in fast muscles. This is consistent with previous studies which show that myostatin is preferentially expressed in fast muscle fibers, and myostatin null mice exhibit primarily fast-twitch fiber hypertrophy (Carlson et al., 1999) similar to double-muscled cattle (Wegner et al., 2000; Deveaux et al., 2003).

Creatine and creatine kinase

Results from microarray and RT-PCR analyses would suggest differences in creatine content between MKO mice and WT mice. Past studies have used creatine and creatinine in the blood as a marker for double-muscled cattle (Hanset R. and Michaux C.,

1982), further supporting this assumption. Expression of *Gamt* was increased in MKO mice compared with WT mice ($P<0.05$), but expression data reveals little regarding enzyme activity. Thus, creatine content, the end product of the reaction catalyzed by GAMT, was measured directly in TA and GAS muscles. Creatine content of MKO mice was increased ($P<0.001$) nearly 40% compared with WT mice (Table 3.3). The TA had slightly higher creatine content than the GAS muscle ($P=0.102$), but there was no interaction of muscle and genotype for creatine content. During intense contraction, fast muscle fibers exhibit large ATP depletions while slow muscle fibers do not (Meyer and Terjung, 1979), therefore slow muscles have a lower requirement for immediate replenishment of ATP. Therefore, the increased creatine content in TA compared with GAS muscle may be secondary to fiber type composition. Similarly, increased creatine content in MKO mice may also be related to the shift in fiber type. This could be confirmed by measuring creatine content of individual fast muscle fibers compared with individual slow fibers.

Research demonstrates that creatine synthesis occurs primarily in the liver and kidneys (Sandberg et al., 1953). However, the contribution of other tissues, including skeletal muscle and brain, to creatine synthesis is uncertain. It is generally assumed that a creatine transporter is responsible for uptake of creatine into tissues such as skeletal muscle, cardiac muscle, and brain; however, recent studies have suggested that the brain is capable of producing its own creatine because *Gatm* and *Gamt* are expressed in this tissue (Braissant et al., 2001). Confirmed expression of *Gatm* and *Gamt* in skeletal muscle in this study and others (Braissant et al., 2005) would suggest that skeletal muscle also synthesizes creatine. However, it would be interesting to also measure creatine

uptake and expression of the creatine transporter in MKO mice to confirm that increased creatine synthesis is responsible for increased creatine content in these animals.

Creatine binds to phosphate, forming phosphocreatine (PCr). Sudden energy demands result in the de-phosphorylation of ATP to ADP. Phosphocreatine donates its phosphate to ADP to renew the ATP lost and produce energy. The enzyme responsible for the phosphorylation of creatine is CK. Increased CK activity in MKO mice compared with WT mice (P=0.10) was observed in this study. Creatine kinase activity of myostatin null mice was 919.96 U/gram of muscle compared with 855.25 U/gram of muscle in wild type mice (Table 3.3). While not statistically significant (P=0.145), CK activity of TA was 916.23 U/gram while CK activity of GAS was 858.98U/ gram of muscle tissue. Consistent with the functional demand placed on the muscle, increased CK activity was expected in faster muscles such as the TA. Fast muscles have an increased demand for ATP replenishment (Meyer and Terjung, 1979) and possess more total creatine and phosphocreatine than slow muscles (Brault and Terjung, 2003; Murphy et al., 2001).

Conclusions

The main objective of this experiment was to confirm the results of previous microarray analysis which suggested that lack of functional myostatin altered numerous biological processes in MKO mice compared with WT mice. We previously described those biological processes and individual genes involved in each process. The results of that experiment were limited to the fast TA muscle, however, so we investigated the same genes in GAS, and SOL muscles. Genes from all muscles showed fairly consistent changes in gene expression- aside from *Vldlr* and *Il-15*.

Typical of myostatin mutant animals, body and muscle weights were increased in MKO mice compared with WT mice, with the exception of the SOL muscle. No significant differences in gene expression were observed in the MKO mice compared with the WT mice but this may be partially attributed to the limited sample size of SOL muscle. Similar changes in gene expression were observed in this muscle compared with the other two muscles despite the lack of physiologically response in SOL muscle weight. Conversely, the SOL muscle was unresponsive to changes in gene expression of MHC isoforms typically associated with the myostatin null mutation. This suggests slow muscle gene expression may be altered with the lack of myostatin function though the effect on muscle weigh is limited.

Microarray analysis also indicated increased expression of the two enzymes responsible for creatine biosynthesis, *Gatm* and *Gamt*. Increased expression of *Gamt* was further confirmed by RT-PCR, suggesting that skeletal muscles are capable of synthesizing their own creatine, and may not be fully dependent on external sources. Creatine content and CK activity was measured directly and was found to be increased in MKO compared with WT mice. We hypothesize that increased fast fiber content of MKO mice results in higher creatine content and CK activity compared with WT mice; a direct result of the fiber type composition and the energy demands of the fast fibers. Future studies should examine the uptake of creatine into skeletal muscles of MKO mice versus WT mice to validate these assumptions.

Literature Cited

Binas, B., and Erol, E. (2007). FABPs as determinants of myocellular and hepatic fuel metabolism. *Molecular and Cellular Biochemistry, 299*, 75-84.

Binas, B., Danneberg, H., McWhir, J., Mullins, L., and Clark, A. J. (1999). Requirement for the heart-type fatty acid binding protein in cardiac fatty acid utilization. *The FASEB Journal, 13*, 805-812.

Braissant, O., Henry, H., Loup, M., Eilers, B., and Bachmann, C. (2001). Endogenous synthesis and transport of creatine in the rat brain: An in situ hybridization study. *Molecular Brain Research, 86*, 193-201.

Braissant, O., Henry, H., Villard, A., Speer, O., Wallimann, T., and Bachmann, C. (2005). Creatine synthesis and transport during rat embryogenesis: Spatiotemporal expression of AGAT, GAMT and CT1. *BMC Developmental Biology, 5*, 9-25.

Brault, J. J., and Terjung, R. L. (2003). Creatine uptake and creatine transporter expression among rat skeletal muscle fiber types. *American Journal of Physiology - Cell Physiology, 284*, C1481-C1489.

Carlson, C. J., Booth, F. W., and Gordon, S. E. (1999). Skeletal muscle myostatin mRNA expression is fiber-type specific and increases during hindlimb unloading. *American Journal of Physiology- Regulatory, Integrative and Comparative Physiology, 277*, 601-606.

Charlier, C., Segers, K., Wagenaar, D., Karim, L., Berghmans, S., Jaillon, O., Shay, T., Weissenbach, J., Cockett, N., Gyapay, G., and Georges, M. (2001). Human-ovine comparative sequencing of a 250-kb imprinted domain encompassing the callipyge (clpg) locus and identification of six imprinted transcripts: DLK1, DAT, GTL2, PEG11, antiPEG11, and MEG8. *Genome Research, 11*, 850-862.

Coburn, C. T., Knapp, Jr. F. F., Febbraio, M., Beets, A. L., Silverstein, R. L., and Abumrad, N.A. (2000). Defective uptake and utilization of long-chain fatty acids in muscle and adipose tissues of CD36 knockout mice. *Journal of Biological Chemistry, 275*, 32523-32529.

DeChiara, T. M., Efstratiadis, A., and Robertsen, E. J. (1990). A growth-deficiency phenotype in heterozygous mice carrying an insulin-like growth factor II gene disrupted by targeting. *Nature, 345*, 78-80.

Deveaux, Véronique, Picard, B., Bouley, J., and Isabelle Cassar-Malek. (2003). Location of myostatin expression during bovine myogenesis in vivo and in vitro. *Reproduction Nutrition Development, 43*, 527-542.

Florini, J. R., Ewton, D. Z., and Roof, S. L. (1991). Insulin-like growth factor-I stimulates terminal myogenic differentiation by induction of myogenin gene expression. *Molecular Endocrinology, 5*, 718-724.

Frykman, P. K., Brown, M. S., Yamamoto, T., Goldstein, J. L., and Herz, J. (1995). Normal plasma lipoproteins and fertility in gene-targeted mice homozygous for a disruption in the gene encoding very low density lipoprotein receptor. *Proceedings of the National Academy of Sciences, 92*, 8453-8457.

Gerrard, D. E., and Grant, A. L. (1994). Insulin-like growth factor-II expression in developing skeletal muscle of double muscled and normal cattle. *Domestic Animal Endocrinology, 11*, 339-347.

Girgenrath, S., Song, K., and Whittemore, L. A. (2005). Loss of myostatin expression alters fiber-type distribution and expression of myosin heavy chain isoforms in slow- and fast-type skeletal muscle. *Muscle and Nerve, 31*, 34-40.

Hanset R., and Michaux C. (1982). Creatine and creatinine levels in plasma red cells and muscles as characteristics of double-muscled cattle. In W. B. King, and F. Menissier (Ediotors), *Muscle hypertrophy of genetic origin and its use to improve beef production* (237-256). The Hague: Martinus Nijhoff Publishers.

Haugk, K. L., Roeder, R. A., Garber, M. J., and Schelling, G. T. (1995). Regulation of muscle cell proliferation by extracts from crushed muscle. *Journal of Animal Science, 73*, 1972-1981.

Ibrahimi, A., Bonen, A., Blinn, W., Hajri, T., Li, X., Zhong, K., Cameron, R., and Abumrad, N.A. (1999). Muscle-specific overexpression of FAT/CD36 enhances fatty acid oxidation by contracting muscle, reduces plasma triglycerides and fatty acids, and increases plasma glucose and insulin. *Journal of Biological Chemistry, 274*, 26761-26766.

Leighton, P. A., Ingram, R. S., Eggenschwiler, J., Efstratiadis, A., and Tilghman, S. M. (1995). Disruption of imprinting caused by deletion of the H19 gene region in mice. *Nature, 375*, 34-39.

Listrat, A., Belair, L., Picard, B., Boulle, N., Geay, Y., and Djiane, J. (1999). Insulin-like growth factor II (IGF-II) mRNA expression during skeletal muscle development of double-muscled and normal bovine foetuses. *Reproduction, Nutrition, Development, 39*(1), 113-124.

Livak, K. J., and Schmittgen, T. D. (2001). Analysis of relative gene expression data using real-time quantitative PCR and the $2^{-\Delta\Delta CT}$ method. *Methods, 25*, 402-408.

Meyer, R. A., and Terjung, R. L. (1979). Differences in ammonia and adenylate metabolism in contracting fast and slow muscle. *American Journal of Physiology - Cell Physiology, 237*, C111-C118.

Miyoshi, N., Wagatsuma, H., Wakana, S., Shiroishi, T., Nomura, M., Aisaka, K., Kohda, T., Surani, M.A., Kaneko-Ishino, T., and Ishino, F. (2000). Identification of an imprinted gene, Meg3/Gtl2 and its human homologue MEG3, first mapped on mouse distal chromosome 12 and human chromosome 14q. *Genes to Cells, 5*, 211-220.

Murphy, R., McConell, G., Cameron-Smith, D., Watt, K., Ackland, L., Walzel, B., Wallimann, T., and Snow, R. (2001). Creatine transporter protein content, localization, and gene expression in rat skeletal muscle. *American Journal of Physiology - Cell Physiology, 280*, C415-C422.

Pirskanen, A., Kiefer, J. C., and Hauschka, S. D. (2000). IGFs, insulin, SHH, bFGF, and TGF-β1 interact synergistically to promote somite myogenesis in vitro. *Developmental Biology, 224*, 189-203.

Quinn, L. S., Anderson, B. G., Strait-Bodey, L., Stroud, A. M., and Argiles, J. M. (2009). Oversecretion of interleukin-15 from skeletal muscle reduces adiposity. *American Journal of Physiology - Endocrinology and Metabolism, 296*, E191-E202.

Quinn, L., Haugk, K., and Grabstein, K. (1995). Interleukin-15: A novel anabolic cytokine for skeletal muscle. *Endocrinology, 136*, 3669-3672.

Sandberg, A. A., Hecht, H. H., and Tyler, F. H. (1953). Studies in disorders of muscle. X. the site of creatine synthesis in the human. *Metabolism, 2*, 22-29.

Steelman, C. A., Recknor, J. C., Nettleton, D., and Reecy, J. M. (2006). Transcriptional profiling of myostatin-knockout mice implicates Wnt signaling in postnatal skeletal muscle growth and hypertrophy. *The FASEB Journal, 20*, 580-582.

Takahashi, S., Suzuki, J., Kohno, M., Oida, K., Tamai, T., Miyabo, S., Yamamoto, T; and Nakai, T. (1995). Enhancement of the binding of triglyceride-rich lipoproteins to the very low density lipoprotein receptor by apolipoprotein E and lipoprotein lipase. *Journal of Biological Chemistry, 270*, 15747-15754.

Tiebel, O., Oka, K., Robinson, K., Sullivan, M., Martinez, J., Nakamuta, M., Ishimura-Oka, K., and Chan, L. (1999). Mouse very low-density lipoprotein receptor (VLDLR): Gene structure, tissue-specific expression and dietary and developmental regulation. *Atherosclerosis, 145*, 239-251.

Wegner, J., Albrecht, E., Fiedler, I., Teuscher, F., Papstein, H. J., and Ender, K. (2000). Growth- and breed-related changes of muscle fiber characteristics in cattle. *Journal of Animal Science, 78*, 1485-1496.

Weinstock, P. H., Levak-Frank, S., Hudgins, L. C., Radner, H., Friedman, J. M., Zechner, R., and Breslow, J. L. (1997). Lipoprotein lipase controls fatty acid entry into adipose tissue, but fat mass is preserved by endogenous synthesis in mice deficient in adipose tissue lipoprotein lipase. *Proceedings of the National Academy of Sciences, 94*, 10261-10266.

Wyss, M., and Kaddurah-Daouk, R. (2000). Creatine and creatinine metabolism. *Physiological Reviews, 80*, 1107-1213.

Zhou, Y., Zhong, Y., Wang, Y., Zhang, X., Batista, D. L., Gejman, R., Ansell, P.J., Zhao, J., Weng, C., and Klibanski, A. (2007). Activation of p53 by MEG3 non-coding RNA. *Journal of Biological Chemistry, 282*, 24731-24742.

Table 3.1. Primers used for RT-PCR. Fold Changes (FC) and P-values are from previous microarray analysis.

Symbol	Product	Genebank Accession	TaqMan Assay ID	FC	*P*value
Igf2	insulin-like growth factor 2	NM_010514	Mm00439565_g1	2.44	0.04
Meg3	Gtl2, imprinted maternally expressed untranslated mRNA	NM_144513	Mm00522599_m1	2.96	0.11
Gamt	guanidinoacetate methyltransferase	NM_010255	Mm00487473_m1	1.52	0.07
Cd36	CD36 antigen	NM_007643	Mm01135198_m1	0.58	0.07
Vldlr	very low density lipoprotein receptor	NM_013703	Mm00443281_m1	0.57	0.07
Il15	interleukin 15	NM_008357	Mm00434210_m1	0.61	0.09
Lpl	lipoprotein lipase	NM_008509	Mm00434764_m1	0.54	0.04
Fabp3	fatty acid binding protein 3, muscle and heart	NM_010174	Mm02342494_m1	0.43	0.07
Myh1	myosin, heavy polypeptide 1, skeletal muscle, adult	XM_354615	Mm01332489_m1	0.56	0.16
Myh2	myosin, heavy polypeptide 2, skeletal muscle, adult	NM_144961	Mm00454982_m1	0.18	0.10
Myh4	myosin, heavy polypeptide 4, skeletal muscle	XM_126119	Mm01332541_m1	1.42	0.16
Myh7	myosin, heavy polypeptide 7, cardiac muscle, beta	NM_080728	Mm00600555_m1	0.57	0.40
Gapdh	glyceraldehyde-3-phosphate dehydrogenase	NM_008084	Mm99999915_g1	-	-

Table 3.2. Effect of genotype on body weight and individual muscle weights in the myostatin null (MKO) and wild type (WT) mice.

	Genotype			
	WT	MKO	S.E.M.	*P*-value
Number of mice	8	8		
Body Weight (g)	21.28	23.87	0.605	0.009
Muscles				
Biceps Femoris (g)	0.30	0.32	0.012	0.160
Triceps Brachii (g)	0.16	0.29	0.092	<.0001
Gastrocnemius (g)	0.24	0.34	0.127	<.0001
Tibialis Anterior (g)	0.13	0.17	0.007	0.003
Soleus (g)	0.012	0.013	0.001	0.537

Values are lsmeans ± S.E.M.

Table 3.3. Effects of genotype and muscle on creatine content and creatine kinase activity in wild type and myostatin null mice.

	Creatine Content (mg/g)	Creatine Kinase (U/g)
Number of mice	6	6
Genotype		
Wild Type	2.91	855.25
Myostatin Null	3.99	919.96
S.E.M.	0.148	26.75
P-value	<0.0001	0.75
Muscle		
Tibialis Anterior	3.48	916.23
Gastrocnemius	3.41	858.98
S.E.M.	0.148	26.75
P-value	0.102	0.15

Values are lsmeans ± S.E.M.
U=Unit Creatine Kinase where 1 Unit of CK will transfer 1 μmole of phosphate from phosphocreatine to ADP per minute at pH 6.0.

Figure 3.1. Fold change in gene expression of the Tibialis Anterior (A), Gastrocnemius (B), and Soleus (C) muscles in myostatin null (MKO) and wild type (WT) mice. Bars represent least square means ± standard error and * indicates MKO differs from WT ($P < 0.05$).

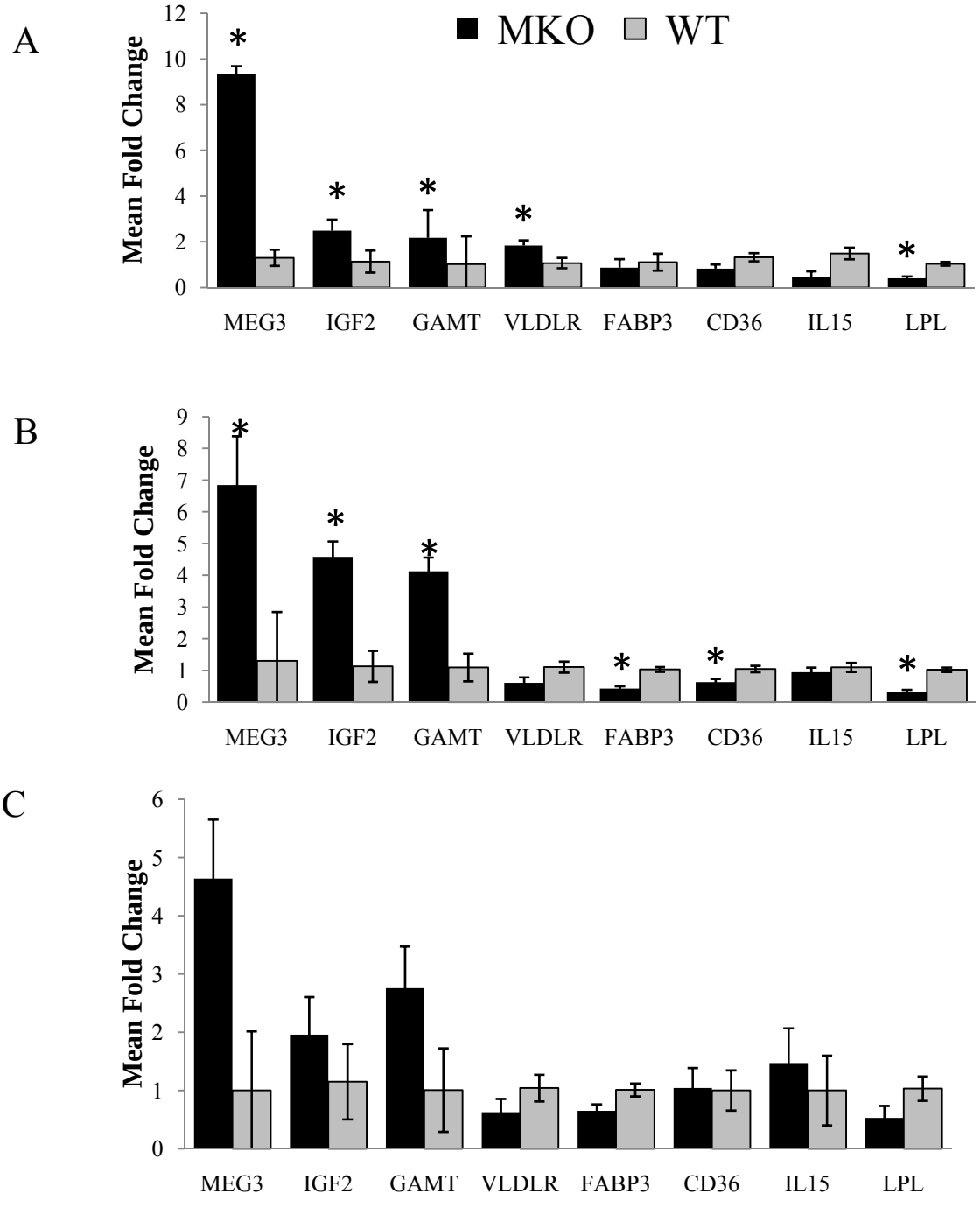
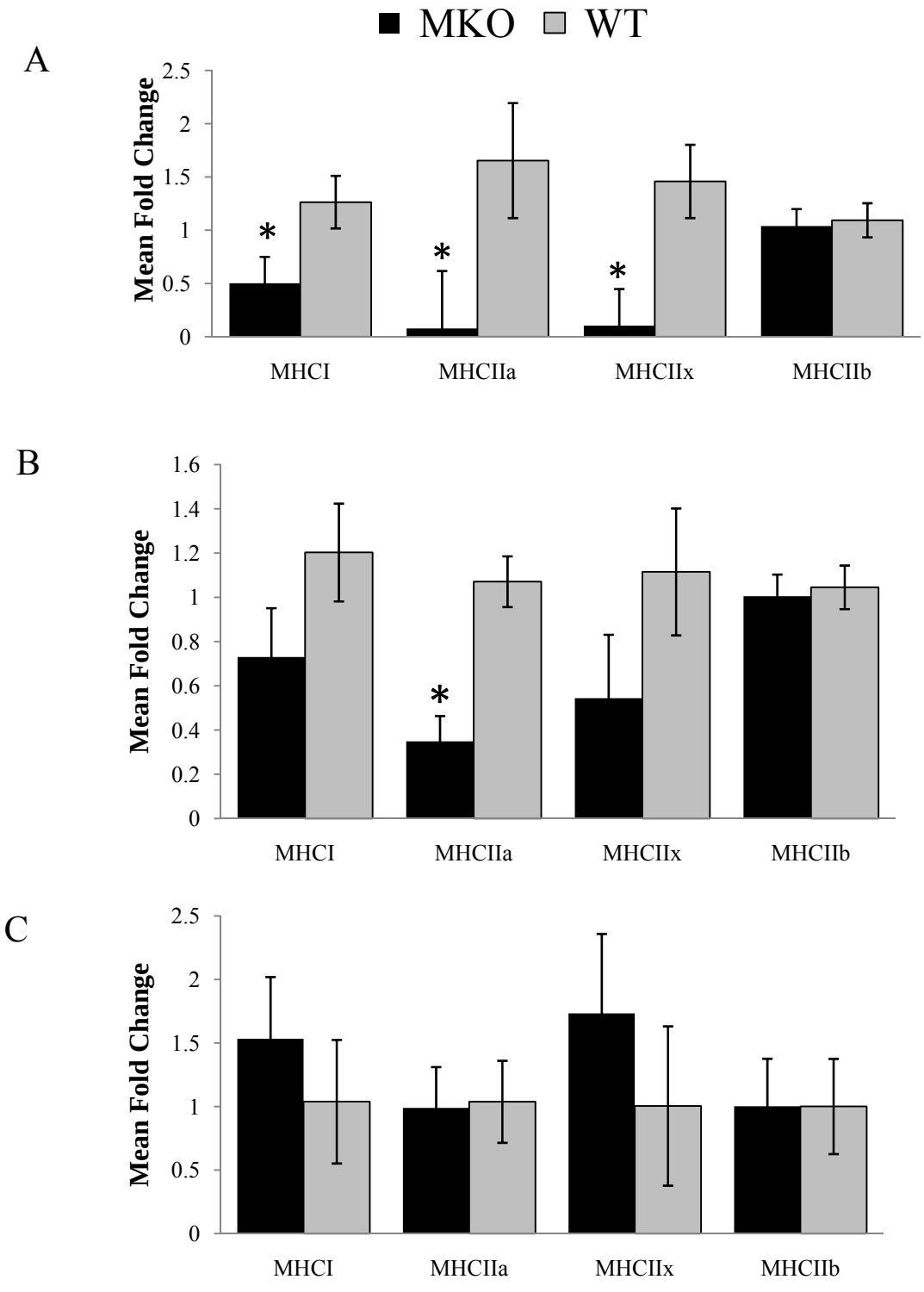


Figure 3.2. Fold change in gene expression of myosin heavy chain isoforms in the Tibialis Anterior, Gastrocnemius, and Soleus muscles of myostatin null(MKO) and wild type (WT) mice. Mean fold change represents least square means ± standard error and * indicates MKO differs from WT ($P < 0.05$).



APPENDIX

List of genes for Gene Ontology Tree Machine Annotation

Symbol	Product	FC	FDR-adj.P.Value
Myh8	myosin, heavy polypeptide 8, skeletal muscle, perinatal	2.25	0.003
1110001A05Rik	Mus musculus RIKEN cDNA 1110001A05 gene (1110001A05Rik), mRNA.	1.80	0.012
Esrrg	estrogen-related receptor gamma	0.57	0.012
Prkg1	protein kinase, cGMP-dependent, type I	0.48	0.013
Mgst1	microsomal glutathione S-transferase 1	0.54	0.013
9630033F20Rik	RIKEN cDNA 9630033F20 gene	0.55	0.015
Myo10	myosin X	1.53	0.028
Wdfy1	WD repeat and FYVE domain containing 1	3.34	0.039
2310042L06Rik	RIKEN cDNA 2310042L06 gene	1.50	0.039
Mybph	myosin binding protein H	2.90	0.043
Cd28	CD28 antigen	2.22	0.043
1110059G02Rik	RIKEN cDNA 1110059G02 gene	1.78	0.043
Itgb1	Mus musculus integrin beta 1 (fibronectin receptor beta) (Itgb1), mRNA.	1.59	0.043
Triobp	Mus musculus TRIO and F-actin binding protein (Triobp), mRNA.	1.56	0.043
Coro2a	coronin, actin binding protein 2A	1.52	0.043
Htr6	5-hydroxytryptamine (serotonin) receptor 6	1.48	0.043
2310061J03Rik	Mus musculus RIKEN cDNA 2310061J03 gene (2310061J03Rik), mRNA.	1.45	0.043
9430063L05Rik	RIKEN cDNA 9430063L05 gene	1.44	0.043
Gdf3	growth differentiation factor 3	1.42	0.043
Foxo3	Mus musculus forkhead box O3 (Foxo3), mRNA.	1.41	0.043
Dach2	dachshund 2 (Drosophila)	0.58	0.043
A530026G17	hypothetical protein A530026G17	0.56	0.043
Lpl	lipoprotein lipase	0.54	0.043
Ldh2	lactate dehydrogenase 2, B chain	0.44	0.043
LOC210321	epididymal protein Av381126	0.35	0.043
Triobp	TRIO and F-actin binding protein	1.47	0.043
4833412C05Rik	RIKEN cDNA 4833412C05 gene	2.55	0.043
Cfl2	Mus musculus cofilin 2, muscle (Cfl2), mRNA.	1.53	0.043
Nr5a2	Mus musculus nuclear receptor subfamily 5, group A, member 2 (Nr5a2), mRNA.	1.49	0.043
Kif17	kinesin family member 17	1.46	0.043
Tom1l2	target of myb1-like 2 (chicken)	1.45	0.043
2210008N01Rik	RIKEN cDNA 2210008N01 gene	1.43	0.043
9130213B05Rik	RIKEN cDNA 9130213B05 gene	1.41	0.043
Gpd1	glycerol-3-phosphate dehydrogenase 1 (soluble)	1.40	0.043
Bhlhb3	basic helix-loop-helix domain containing, class B3	1.40	0.043
Fxyd6	FXYD domain-containing ion transport regulator 6	0.59	0.043
Plac9	placenta specific 9	0.58	0.043
Lpl	lipoprotein lipase	0.54	0.043
Prkg1	protein kinase, cGMP-dependent, type I	0.52	0.043
Igf2	insulin-like growth factor 2	2.44	0.044
Dusp13	dual specificity phosphatase 13	1.56	0.044
C530050O22Rik	RIKEN cDNA C530050O22 gene	1.51	0.044
2410005H09Rik	RIKEN cDNA 2410005H09 gene	1.48	0.044

Renbp	renin binding protein	1.47	0.044
Pvrl3	Mus musculus poliovirus receptor-related 3 (Pvrl3), mRNA.	1.41	0.044
Dlk1	delta-like 1 homolog (Drosophila)	1.41	0.044
Jun	Jun oncogene	1.40	0.044
Ppp1r14c	protein phosphatase 1, regulatory (inhibitor) subunit 14c	1.39	0.044
Lrrn1	leucine rich repeat protein 1, neuronal	0.52	0.044
Grb14	Mus musculus growth factor receptor bound protein 14 (Grb14), mRNA.	0.48	0.044
C130068O12Rik	RIKEN cDNA C130068O12 gene	1.43	0.046
r171.1	Rat cytomegalovirus Maastricht, complete genome.	1.41	0.046
Actc1	actin, alpha, cardiac	1.91	0.047
1110030K22Rik	RIKEN cDNA 1110030K22 gene	0.54	0.047
Cbfa2t1h	Mus musculus CBFA2T1 identified gene homolog (human) (Cbfa2t1h), mRNA.	1.40	0.047
9530064J02	hypothetical protein 9530064J02	2.45	0.048
Hist2h3c2	histone 2, H3c2	1.43	0.048
C3	complement component 3	0.53	0.049
B230312C02Rik	RIKEN cDNA B230312C02 gene	1.95	0.049
Phc2	Mus musculus polyhomeotic-like 2 (Drosophila), mRNA (cDNA clone IMAGE:5321987), complete cds.	1.50	0.051
Fbp2	fructose bisphosphatase 2	1.73	0.051
Ddr1	Mus musculus discoidin domain receptor family, member 1 (Ddr1), mRNA.	1.44	0.051
Gdf8	growth differentiation factor 8	0.11	0.051
4832428D23Rik	RIKEN cDNA 4832428D23 gene	2.25	0.052
6430548M08Rik	MKIAA0513 protein (Fragment).	1.81	0.055
0610041G09Rik	RIKEN cDNA 0610041G09 gene	1.67	0.055
1110012O05Rik	RIKEN cDNA 1110012O05 gene	1.66	0.055
8030402F09Rik	RIKEN cDNA 8030402F09 gene	1.65	0.055
6430548M08Rik	RIKEN cDNA 6430548M08 gene	1.60	0.055
Banp	Btg3 associated nuclear protein	1.52	0.055
Csda	Mus musculus cold shock domain protein A (Csda), mRNA.	1.52	0.055
Catnbip1	catenin beta interacting protein 1	1.51	0.055
	Mus musculus 13 days embryo head cDNA, RIKEN full-length enriched library, clone:3110005M20 product:serine/arginine-rich protein specific kinase 2, full insert sequence.	1.50	0.055
Mkl1	MKL (megakaryoblastic leukemia)/myocardin-like 1	1.48	0.055
F730017E11Rik	RIKEN cDNA F730017E11 gene	1.48	0.055
1700003N22Rik	RIKEN cDNA 1700003N22 gene	1.47	0.055
Tenc1	Mus musculus tensin like C1 domain-containing phosphatase, mRNA (cDNA clone MGC:47266 IMAGE:4188303), complete cds.	1.43	0.055
Fth1	ferritin heavy chain 1	1.42	0.055
Abca1	ATP-binding cassette, sub-family A (ABC1), member 1	0.61	0.055
1100001H23Rik	RIKEN cDNA 1100001H23 gene	0.53	0.055
Temt	thioether S-methyltransferase	0.44	0.055
Bdh	3-hydroxybutyrate dehydrogenase (heart, mitochondrial)	0.31	0.055
Sfrs2	splicing factor, arginine/serine-rich 2 (SC-35)	1.55	0.057
Ctss	cathepsin S	1.51	0.057
Nrtn	neurturin	1.42	0.057
Bdh	3-hydroxybutyrate dehydrogenase (heart, mitochondrial)	0.36	0.057

Tceal5	transcription elongation factor A (SII)-like 5	1.83	0.057
Hn1	hematological and neurological expressed sequence 1	1.42	0.057
Pdlim7	PDZ and LIM domain 7	1.53	0.058
Wnt4	wingless-related MMTV integration site 4	1.41	0.058
Gab3	growth factor receptor bound protein 2-associated protein 3	1.43	0.061
2310057H16Rik	RIKEN cDNA 2310057H16 gene	1.43	0.061
5230400C17Rik	RIKEN cDNA 5230400C17 gene	0.59	0.061
9130213B05Rik	RIKEN cDNA 9130213B05 gene	1.57	0.063
Wnt2b	Mus musculus wingless related MMTV integration site 2b (Wnt2b), mRNA.	1.52	0.063
Dab2ip	disabled homolog 2 (Drosophila) interacting protein	1.47	0.063
Ent2	Mus musculus equilibrative nitrobenzylthioinosine-insensitive nucleoside transporter ENT2 (Ent2) mRNA, complete cds.	1.47	0.066
Vldlr	very low density lipoprotein receptor	0.57	0.066
Cd36	CD36 antigen	0.58	0.066
Sox6	SRY-box containing gene 6	1.54	0.068
Trp63	transformation related protein 63	1.48	0.068
Gamt	guanidinoacetate methyltransferase	1.52	0.068
Pdlim3	PDZ and LIM domain 3	1.46	0.068
Xlkd1	extra cellular link domain-containing 1	1.42	0.069
Ank1	ankyrin 1, erythroid	1.57	0.069
Mtvr2	mammary tumor virus receptor 2	1.43	0.069
B230106I24Rik	RIKEN cDNA B230106I24 gene	0.60	0.069
Fabp3	fatty acid binding protein 3, muscle and heart	0.43	0.069
D5Ertd593e	DNA segment, Chr 5, ERATO Doi 593, expressed	1.56	0.070
Dctn2	dynactin 2	1.52	0.070
Dctn1	dynactin 1	1.44	0.070
Actc1	actin, alpha, cardiac	2.57	0.071
Peg3	paternally expressed 3	1.54	0.071
Epb4.9	Mus musculus erythrocyte protein band 4.9 (Epb4.9), mRNA.	1.50	0.071
Actb	Mus musculus actin, beta, cytoplasmic (Actb), mRNA.	1.77	0.071
Mg29	mitsugumin 29	1.55	0.071
BC021785	cDNA sequence BC021785	1.51	0.071
Ap1m2	adaptor protein complex AP-1, mu 2 subunit	1.45	0.071
Gadd45a	growth arrest and DNA-damage-inducible 45 alpha	1.43	0.071
Fndc5	fibronectin type III domain containing 5	0.60	0.071
Pdhb	pyruvate dehydrogenase (lipoamide) beta	0.60	0.071
B130052G07Rik	RIKEN cDNA B130052G07 gene	1.59	0.071
Slc16a3	solute carrier family 16 (monocarboxylic acid transporters), member 3	1.54	0.074
Actb	Mus musculus actin, beta, cytoplasmic (Actb), mRNA.	1.63	0.074
Lmod2	leiomodin 2 (cardiac)	0.34	0.074
Rpp14	ribonuclease P 14 subunit (human)	0.50	0.075
Foxd3	forkhead box D3	1.52	0.076
Mb	myoglobin	0.49	0.077
Usp20	ubiquitin specific protease 20	1.51	0.078
Atp6v0a1	ATPase, H+ transporting, lysosomal V0 subunit a isoform 1	1.51	0.078
Myo10	myosin X	1.44	0.078
A330093E20Rik	RIKEN cDNA A330093E20 gene	1.42	0.079

Pbxip1	pre-B-cell leukemia transcription factor interacting protein 1	1.39	0.079
Lrrc2	leucine rich repeat containing 2	0.59	0.079
Rassf5	Ras association (RalGDS/AF-6) domain family 5	1.39	0.081
Lrp6	low density lipoprotein receptor-related protein 6	1.64	0.082
Chd7	chromodomain helicase DNA binding protein 7	1.41	0.084
Myl3	myosin, light polypeptide 3	0.27	0.085
Vgll4	vestigial like 4 (Drosophila)	1.49	0.085
Sap30	sin3 associated polypeptide	1.51	0.086
Il15	interleukin 15	0.61	0.087
Mrps26	mitochondrial ribosomal protein S26	1.43	0.087
Tln	Mus musculus talin (Tln), mRNA.	1.56	0.087
Mafb	v-maf musculoaponeurotic fibrosarcoma oncogene family, protein B (avian)	0.54	0.087
Emp1	epithelial membrane protein 1	1.63	0.087
1700039I01Rik	RIKEN cDNA 1700039I01 gene	1.43	0.087
2700082O15Rik	RIKEN cDNA 2700082O15 gene	0.47	0.087
Atp1b1	ATPase, Na+/K+ transporting, beta 1 polypeptide	0.51	0.088
9630033F20Rik	RIKEN cDNA 9630033F20 gene	1.68	0.092
4930438M06Rik	Mus musculus RIKEN cDNA 4930438M06 gene (4930438M06Rik), mRNA.	1.46	0.093
B430320C24Rik	RIKEN cDNA B430320C24 gene	1.83	0.093
Gatm	glycine amidinotransferase (L-arginine:glycine amidinotransferase)	1.66	0.093
Amd1	S-adenosylmethionine decarboxylase 1	0.52	0.093
Atp2a1	ATPase, Ca++ transporting, cardiac muscle, fast twitch 1	1.49	0.094
Adamts4	a disintegrin-like and metalloprotease (reprolysin type) with thrombospondin type 1 motif, 4	1.42	0.094
Fabp4	fatty acid binding protein 4, adipocyte	0.60	0.096
Tceal7	transcription elongation factor A (SII)-like 7	1.78	0.097
Ddc	dopa decarboxylase	1.45	0.097
9530003J23Rik	RIKEN cDNA 9530003J23 gene	0.56	0.098
Spon2	spondin 2, extracellular matrix protein	1.99	0.098
BC035954	cDNA sequence BC035954	1.39	0.098
Atp1b1	ATPase, Na+/K+ transporting, beta 1 polypeptide	0.40	0.098
Zmynd17	zinc finger, MYND domain containing 17	2.81	0.099
AW822216	expressed sequence AW822216	1.53	0.099
2310007D09Rik	RIKEN cDNA 2310007D09 gene	1.47	0.099
Myh2	myosin, heavy polypeptide 2, skeletal muscle, adult	0.18	0.099
6430514B01	hypothetical protein 6430514B01	1.53	0.100
Gng2	guanine nucleotide binding protein (G protein), gamma 2 subunit	1.68	0.100
Prkag2	protein kinase, AMP-activated, gamma 2 non-catalytic subunit	1.43	0.100
Pdhb	pyruvate dehydrogenase (lipoamide) beta	0.44	0.100
Fmod	fibromodulin	1.75	0.101
Mapre3	microtubule-associated protein, RP/EB family, member 3	1.49	0.102
Gbp5	guanylate nucleotide binding protein 5	0.59	0.102
Emid2	EMI domain containing 2	1.41	0.103
Nfic	nuclear factor I/C	1.47	0.104
Gtl2	GTL2, imprinted maternally expressed untranslated mRNA	2.96	0.105

6720458D17Rik	RIKEN cDNA 6720458D17 gene	1.81	0.106
1110033O09Rik	RIKEN cDNA 1110033O09 gene	1.40	0.106
Klk16	kallikrein 16	1.58	0.107
Pde4b	phosphodiesterase 4B, cAMP specific	1.42	0.107
Slc16a6	solute carrier family 16 (monocarboxylic acid transporters), member 6	1.47	0.107
Pabpc1	poly A binding protein, cytoplasmic 1	1.41	0.108
Chrna1	cholinergic receptor, nicotinic, alpha polypeptide 1 (muscle)	1.55	0.108
C130027E04Rik	RIKEN cDNA C130027E04 gene	1.42	0.108
Actn3	actinin alpha 3	1.68	0.109
0610025O11Rik	RIKEN cDNA 0610025O11 gene	1.68	0.109
Myom3	myomesin family, member 3	0.51	0.110
9830123M21Rik	RIKEN cDNA 9830123M21 gene	1.92	0.112
Capns1	calpain, small subunit 1	1.46	0.112
Bin1	bridging integrator 1	1.48	0.113
Kcnc4	potassium voltage gated channel, Shaw-related subfamily, member 4	1.42	0.113
Six2	sine oculis-related homeobox 2 homolog (Drosophila)	1.42	0.114
Lass1	longevity assurance homolog 1 (S. cerevisiae)	1.43	0.116
2700038N03Rik	RIKEN cDNA 2700038N03 gene	1.41	0.117
Vim	Mus musculus vimentin (Vim), mRNA.	1.39	0.118
A930008A22Rik	RIKEN cDNA A930008A22 gene	1.48	0.124
Myoz2	myozenin 2	0.51	0.125
Klk13	kallikrein 13	1.47	0.125
Myh3	myosin, heavy polypeptide 3, skeletal muscle, embryonic	0.59	0.129
Col16a1	procollagen, type XVI, alpha 1	1.41	0.130
4832441B07Rik	RIKEN cDNA 4832441B07 gene	2.24	0.131
Alb1	albumin 1	4.07	0.133
Ddc	dopa decarboxylase	1.46	0.133
Ckap4	cytoskeleton-associated protein 4	1.40	0.133
Smad7	MAD homolog 7 (Drosophila)	1.55	0.134
Col1a1	procollagen, type I, alpha 1	1.67	0.134
Nfix	nuclear factor I/X	1.40	0.136
Gse1	genetic suppressor element 1	1.61	0.137
Phlda1	pleckstrin homology-like domain, family A, member 1	1.40	0.141
Rian	RNA imprinted and accumulated in nucleus	2.31	0.141
Gstm1	glutathione S-transferase, mu 1	1.40	0.142
Fabp1	fatty acid binding protein 1, liver	2.33	0.143
Ddit4l	DNA-damage-inducible transcript 4-like	1.54	0.145
H19	H19 fetal liver mRNA	1.91	0.149
Nov	nephroblastoma overexpressed gene	1.43	0.151
Bace1	beta-site APP cleaving enzyme 1	1.56	0.152
Ktn1	kinectin 1	2.00	0.155
AI839562	expressed sequence AI839562	1.44	0.158
Hoxa11	homeo box A11	1.58	0.159
Myh4	myosin, heavy polypeptide 4, skeletal muscle	1.42	0.160
Tnfrsf19l	tumor necrosis factor receptor superfamily, member 19-like	1.39	0.161
Csrp3	cysteine and glycine-rich protein 3	0.39	0.163
1110028C15Rik	RIKEN cDNA 1110028C15 gene	0.60	0.163
Myh1	myosin, heavy polypeptide 1, skeletal muscle, adult	0.56	0.163

mt-Nd1	NADH dehydrogenase 1, mitochondrial	0.54	0.163
6330500D04Rik	RIKEN cDNA 6330500D04 gene	1.48	0.164
Kazald1	Kazal-type serine protease inhibitor domain 1	1.65	0.164
Gas1	growth arrest specific 1	1.39	0.165
Nme7	Mus musculus non-metastatic cells 7, protein expressed in (Nme7), mRNA.	0.42	0.166
Nr4a2	nuclear receptor subfamily 4, group A, member 2	1.41	0.166
Lgals3	lectin, galactose binding, soluble 3	1.98	0.167
Nfil3	nuclear factor, interleukin 3, regulated	1.57	0.167
Cxcl4	chemokine (C-X-C motif) ligand 4	1.51	0.172
Tph1	tryptophan hydroxylase 1	1.68	0.173
Dkk3	dickkopf homolog 3 (Xenopus laevis)	1.78	0.177
1500015O10Rik	RIKEN cDNA 1500015O10 gene	1.55	0.177
Smyd2	SET and MYND domain containing 2	1.41	0.178
2310065F04Rik	RIKEN cDNA 2310065F04 gene	1.45	0.179
Pigt	phosphatidylinositol glycan, class T	1.45	0.179
Jarid1d	jumonji, AT rich interactive domain 1D (Rbp2 like)	0.60	0.182
Prg4	proteoglycan 4 (megakaryocyte stimulating factor, articular superficial zone protein)	1.55	0.183
	Mus musculus tropomyosin 3 mRNA, complete cds.	0.50	0.183
2410003B16Rik	RIKEN cDNA 2410003B16 gene	1.53	0.185
Grem2	gremlin 2 homolog, cysteine knot superfamily (Xenopus laevis)	1.59	0.186
Mup3	major urinary protein 3	1.76	0.187
Ambp	alpha 1 microglobulin/bikunin	1.53	0.187
B830012L14Rik	RIKEN cDNA B830012L14 gene	2.04	0.189
Ttr	transthyretin	2.14	0.192
Serpina1a	serine (or cysteine) proteinase inhibitor, clade A, member 1a	1.56	0.193
1810011O10Rik	RIKEN cDNA 1810011O10 gene	0.55	0.194
C630041L24Rik	RIKEN cDNA C630041L24 gene	1.71	0.195
Mup1	major urinary protein 1	2.09	0.199
Mup2	major urinary protein 2	2.43	0.204
Eif2s3y	eukaryotic translation initiation factor 2, subunit 3, structural gene Y-linked	0.36	0.205
F13a1	coagulation factor XIII, A1 subunit	1.46	0.205

AUTHOR'S BIOGRAPHY

Savannah Rihannon-Rose Gabriel, born August 7, 1985, is the youngest child of Steve and Angie Pinkel of O'Fallon, Illinois. She has two sisters, Nicole and Chelsea, and one brother, Aaron. Soon after her 18th birthday, Savannah moved to Champaign, Illinois where she earned a B.S. degree in Animal Sciences from the University of Illinois in 2007. Following graduation, she began graduate school in the University of Illinois Meat Science Laboratory. After completing her M.S. degree in October 2009 under the guidance of Dr. John Killefer, she plans to move to North Carolina to start a new chapter of her life with her fiancé, Sean Holmer.